11
Regulation of Muscle Glycogen Phosphorylase by Physiological Effectors

NATALIA A. CHEBOTAREVA*, SERGEY V. KLINOV AND BORIS I. KURGANOV

A.N. Bakh Institute of Biochemistry, Russian Academy of Sciences, Leninsky prospekt 33, Moscow 117071, Russian Federation

Introduction

Glycogen phosphorylase (1,4-α-D-glucan:orthophosphate glycosyltransferase, EC 2.4.1.1) catalyzes the reversible phosphorolytic cleavage of the α-1,4-glycosidic bonds at the non-reducing ends of the side-chains of glycogen resulting in the formation of glucose-1-P:

$$(\alpha\text{-1,4-glycoside})_n + \text{orthophosphate} = (\alpha\text{-1,4-glycoside})_{n-1} + \alpha\text{-glucose-1-phosphate.} \quad (11.1)$$

The enzyme from rabbit skeletal muscle contains 842 amino acid residues and the essential cofactor pyridoxal-5'-phosphate is linked through its aldehyde group to the ε-amino group of Lys680. The polypeptide chain can be divided in two domains, both of them having a β-sheet core surrounded by α-helices. The main oligomeric form of the enzyme is a dimer. The interactions between identical subunits are relatively few in dephosphorylated form of the enzyme (phosphorylase *b*). The main contacts involve the cap (residues 36 to 45) and the tower (residues 260 to 276) of symmetry-related subunits. X-ray crystallographic studies reveal four ligand-binding sites: catalytic site, allosteric effector site, glycogen storage site, and nucleoside inhibitor site (*Figure 11.1*). The catalytic site is buried in the centre of the subunit where the domains come together. Access to this site is achieved through a narrow channel which is some 1.2 nm long. The access is restricted mostly by the 280s loop (residues 282 to 286). The residues from the 280s loop are displaced upon transition to catalytically active state following motion of the symmetry-related towers. The allosteric effector site is located near the subunit interface and is separated by a distance of 3.2 nm from the catalytic site. The glycogen storage site is 3.0 nm apart from the catalytic site and at a distance of 4.0 nm from the allosteric effector site. The

*To whom correspondence should be addressed (univers@orc.ru)

Abbreviation used: glucose-1-P, glucose 1-phosphate

Biotechnology and Genetic Engineering Reviews – Vol. 18, July 2001
0264–8725/01/18/265–297 $20.00 + $0.00 © Intercept Ltd. P.O. Box 716, Andover, Hampshire SP10 1YG, U.K.

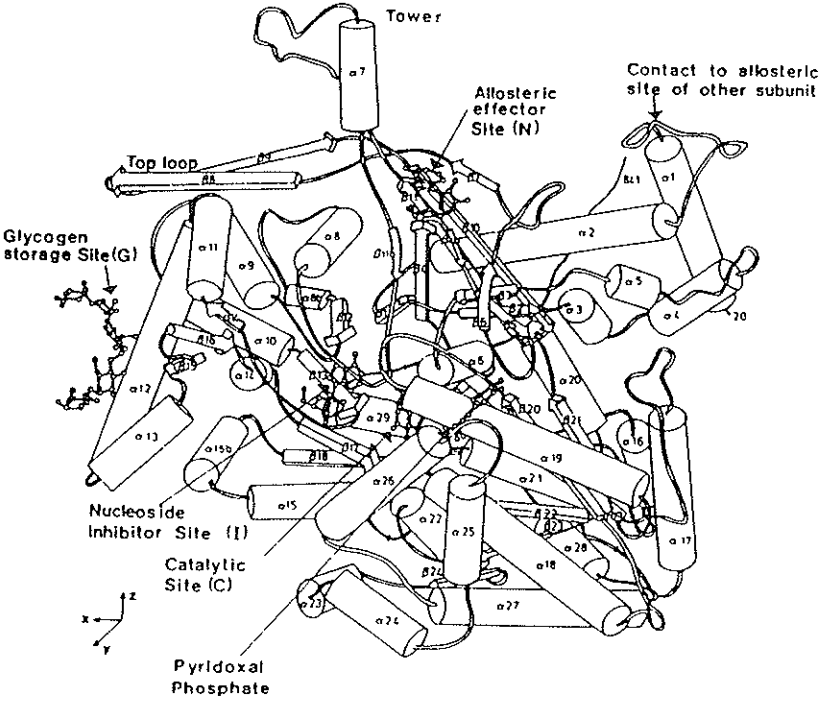

Figure 11.1. A schematic ribbon diagram of phosphorylase *b* viewed down the crystallographic y axis. α-Helices and β-strands are represented by cylinders and arrows respectively (reprinted with permission from Oikonomakos *et al.*, 1992).

nucleoside inhibitor site is located between the domains at the entrance to the catalytic site channel and is formed mainly from the side-chains of Phe285 and Tyr613 which belong to different domains of the enzyme subunit. Displacement of the 280s loop prevents binding in the nucleoside inhibitor site. Among various heterocyclic compounds, flavins show the highest affinity for the nucleoside inhibitor site (Klinova *et al.*, 1988). The enzymatic properties and crystal structure of phosphorylase *b* have been reviewed recently (Johnson *et al.*, 1992; Oikonomakos *et al.*, 1992; Kurganov *et al.*, 1994a; Livanova and Kornilaev, 1996).

In this review we will consider the mechanisms of regulation of muscle phosphorylase *b* which are realized with the participation of cellular metabolites (substrates, allosteric effectors) as well as through enzymatic deimination of the enzyme.

Kinetic mechanism of the allosteric activation of muscle phosphorylase *b* by adenosine 5'-monophosphate

Phosphorylase *b* exhibits a catalytic activity in the presence of the allosteric activator adenosine 5'-monophosphate (AMP). The activatory action of AMP does not follow the hyperbolic law: the dependence of the enzyme activity on AMP concentration is non-linear in the reciprocal plot (Helmreich and Cori, 1964). The experimental dependencies of the initial steady-state rate of the reaction catalyzed by rabbit muscle phosphorylase *b* on the glucose-1-P concentration are also non-linear in reciprocal

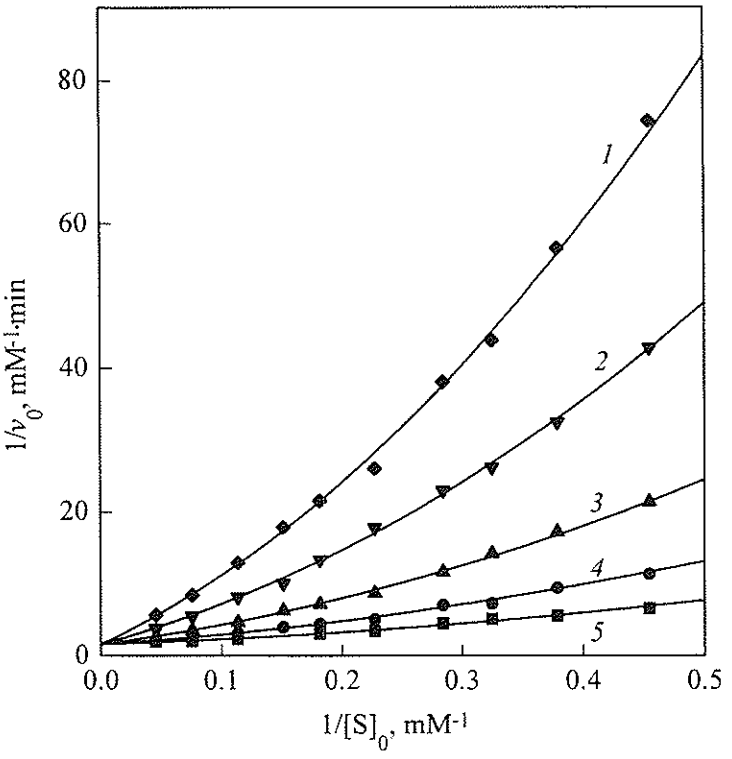

Figure 11.2. The dependence of the initial steady-state rate of the enzymatic reaction catalyzed by phosphorylase *b* on the glucose-1-P concentration in the presence of 1 g/l glycogen at fixed concentrations of AMP (mM): 0.04 (*1*), 0.06 (*2*), 0.1 (*3*), 0.2 (*4*), and 1.0 (*5*). 50 mM glycylglycine buffer, pH 6.8; 0.2 mM EDTA, 0.3 M KCl, 30°C. Points are experimental data; solid lines are calculated according to the kinetic scheme shown in *Figure 11.3* at the following values of parameters: $k = 89$ s^{-1}, $K_{a1} = 0.22$ mM, $K_{a2} = 0.09$ mM, $K_{s1} = 4.4$ mM, $K_{s2} = 1.5$ mM, $[E]_0 = 59$ nM (Klinov and Kurganov, 1994).

coordinates (*Figure 11.2*). These dependencies were obtained at various fixed concentrations of AMP indicated in the legend to the *Figure 11.2*. The non-linear dependencies of the initial steady-state rate of the reaction catalyzed by rabbit muscle phosphorylase *b* on the glucose-1-P concentration in Scatchard coordinates were found by Kastenschmidt *et al.* (1968). The non-linear character of these plots is indicative of the non-hyperbolic kinetics of phosphorylase *b* action. The empirical Hill equation (see Kurganov, 1982) was used to characterize the phosphorylase *b* kinetics. The value of the Hill coefficient for glucose-1-P does not appear to depend on the concentration of the AMP (Klinov and Kurganov, 1994). The average value of the Hill coefficient for glucose-1-P is equal to 1.4. The fact that the Hill coefficient exceeds unity is indicative of the positive kinetic cooperativity between substrate-binding sites in the dimeric enzyme molecule. Similarly, the value of the Hill coefficient for AMP does not appear to depend on the chosen concentration of glucose-1-P. The average value of the Hill coefficient for AMP is equal to 1.6. The fact that the Hill coefficient exceeds unity is indicative of the positive kinetic cooperativity between activator-binding sites in the dimeric molecule of phosphorylase *b*. Similar values for the Hill coefficient for glucose-1-P and AMP have been obtained also by Madsen and Shechosky (1967),

Sealock and Graves (1967), Black and Wang (1968), and Oikonomakos *et al.* (1979). Thus, the kinetics of rabbit muscle phosphorylase *b* is characterized by the positive homotropic cooperativity between the binding sites in the dimeric enzyme molecule.

The different variants of the model proposed by Monod, Wyman and Changeux (1965), which assumes the existence of two conformational states (R and T) of the oligomeric enzyme, were used to describe the kinetics of phosphorylase *b* action. According to the Monod–Wyman–Changeux model the transition between two conformational states of the oligomeric enzyme occurs by the concerted manner. The ligand-binding sites are equivalent and non-interacting in each enzyme state. The conformational states of the enzyme differ in their affinity for ligand and/or in catalytic activity. Kastenschmidt *et al.* (1968) supposed that the catalytic activities of R- and T-states were identical, but the affinities of these states to the ligands were different. Buc and Buc (1968) and Madsen and Shechosky (1967) have suggested that the R-state is active, whilst the T-state is inactive and binds neither substrates nor AMP. Bresler and Firsov (1971) have suggested that T-state is inactive, but has affinity for AMP, whilst the R-state becomes active when two molecules of AMP have been bound. Lowry *et al.* (1967) used a traditional approach to the kinetic study of the enzymatic reaction catalyzed by phosphorylase *b*. They suggested that (i) the binding of one molecule of the ligand affects the binding of the second molecule of the ligand, (ii) the binding of one ligand affects the binding of the other ligand, and (iii) the enzyme reveals a catalytic power exclusively upon the binding with two molecules of AMP and two molecules of inorganic phosphate under the conditions of saturation by glycogen. It should be noted that these authors calculated some parameters of the equation of the enzymatic reaction rate using the graphic methods without any information about the structure of the error of their experiments and without any statistical estimation of the obtained values.

An alternative approach to the kinetic analysis of the allosteric enzymes involves the use of the non-linear regression method for the determination of the parameters of the enzymatic reaction rate equation. Reich *et al.* (1972) used this method to study the kinetics of the enzymatic reaction catalyzed by phosphorylase *b* from pig skeletal muscle. They found that the steady-state kinetics of this reaction were described satisfactorily by the Monod–Wyman–Changeux model involving the catalytically inactive T-state of the enzyme. Kasvinsky *et al.* (1978) used the method of non-linear regression for the analysis of the applicability of seven kinetic models for fitting the steady-state kinetics for the reaction of the lengthening of maltoheptaose saccharide chain catalyzed by glycogen phosphorylase *a* from rabbit skeletal muscles.

Some kinetic models were used for quantitative analysis of the steady-state kinetics of glycogen synthesis catalyzed by phosphorylase *b* from rabbit skeletal muscles under the conditions of saturation of the enzyme by glycogen (Klinov and Kurganov, 1994). Twelve variants of the Monod–Wyman–Changeux model were chosen taking into account the variants of this model proposed by other authors. Klinov and Kurganov analysed some variants of the model involving the interaction of AMP- and glucose-1-P-binding sites. The kinetic model proposed is based on the following assumptions: (i) the independent binding of AMP and one molecule of glucose-1-P with the enzyme saturated by glycogen, (ii) the exclusive binding of the second molecule of glucose-1-P by the enzyme containing two molecules of AMP and one molecule of glucose-1-P, and (iii) the exclusive ability of the complex of the enzyme

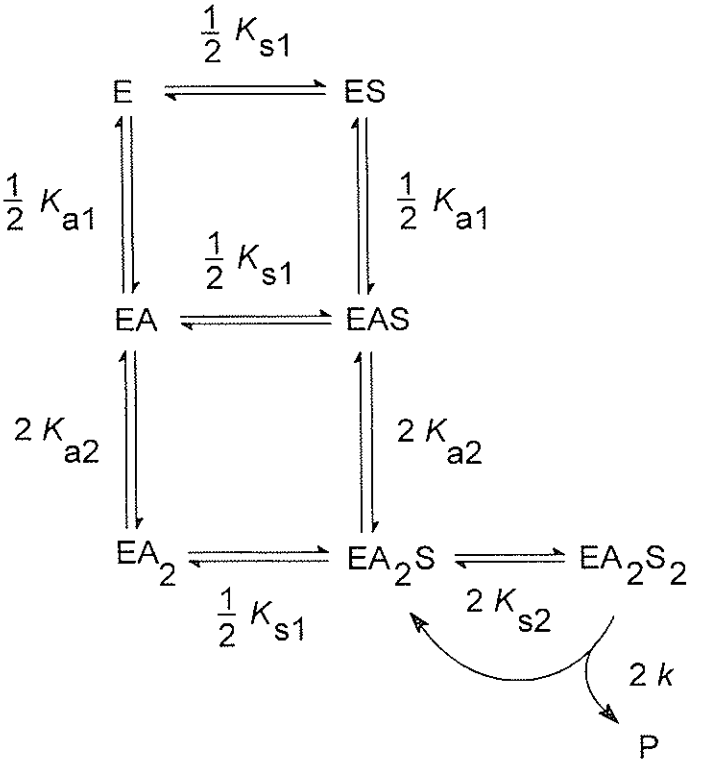

Figure 11.3. The kinetic scheme for the glycogen synthesis catalyzed by glycogen phosphorylase *b* at the saturation by glycogen. The following designations are used: E is the enzyme–glycogen complex, S is glucose-1-P, A is AMP, P is the product(s) of the enzymatic reaction; k is the rate constant for the catalytic transformation of the enzyme–glycogen complex containing two molecules of glucose-1-P and two molecules of AMP; K_{s1} is the dissociation constant for the complex of the enzyme with glycogen and one molecule of glucose-1-P; K_{a1} and K_{a2} are the dissociation constants for the complexes of the enzyme with glycogen and one or two molecules of AMP, respectively; K_{s2} is the dissociation constant for the release of one molecule of glucose-1-P from the complex of the enzyme with glycogen, two molecules of AMP, and two molecules of glucose-1-P (Klinov and Kurganov, 1994).

with glycogen, two molecules of AMP, and two molecules of glucose-1-P to undergo the catalytic transformation. This kinetic scheme is presented in *Figure 11.3*. The parameters of the equation of the initial steady-state rate of the enzymatic reaction were calculated by the non-linear regression method. The proposed kinetic scheme was shown to satisfy the following criteria (Bartfai and Mannervik, 1972): (i) the convergence under the regressional analysis, (ii) the reliability of the values of the parameters of the model, (iii) the minimum of the sum of the weighted squares of the differences between the experimental and calculated values of the reaction rate. The proposed kinetic model allows an adequate description of the experimental dependencies of the initial steady-state rate on glucose-1-P and AMP concentration for the reaction catalyzed by phosphorylase *b* from rabbit skeletal muscles under the conditions of saturation of the enzyme (*Figure 11.2*).

Consider now the possible conformational changes in phosphorylase *b* molecule that are compatible with the proposed kinetic model. The fact that the binding of the

first molecule of AMP results in a decrease in the dissociation constant for the binding of the second molecule of AMP is indicative of the conformational change in the dimeric enzyme molecule induced by AMP. AMP does not affect the binding of the first molecule of glucose-1-P, suggesting that the conformational change in the enzyme induced by AMP does not extend onto the locus of glucose-1-P binding. The fact that the binding of the first molecule of glucose-1-P by the enzyme–glycogen complex containing two molecules of AMP results in a decrease in the dissociation constant for the second molecule of glucose-1-P is indicative of a change in the enzyme conformation induced by substrates and AMP. According to the kinetic scheme presented in *Figure 11.3*, the dimeric enzyme molecule saturated by glycogen acquires the catalytic activity exclusively upon binding of two molecules of AMP and two molecules of glucose-1-P. This fact indicates that phosphorylase *b* is transformed into a catalytically active conformation exclusively upon binding of two molecules of AMP and two molecules of glucose-1-P under the conditions of saturation by glycogen.

The interaction of muscle phosphorylase *b* with flavins

UV- AND VISIBLE-SPECTROPHOTOMETRIC STUDY

Flavins have intrinsic absorbance in the ultraviolet and visible regions of spectrum. Some changes of the absorbance spectrum of flavin mononucleotide (FMN) occur in the presence of muscle phosphorylase *b* (*Figure 11.4*). The portion of protein-bound

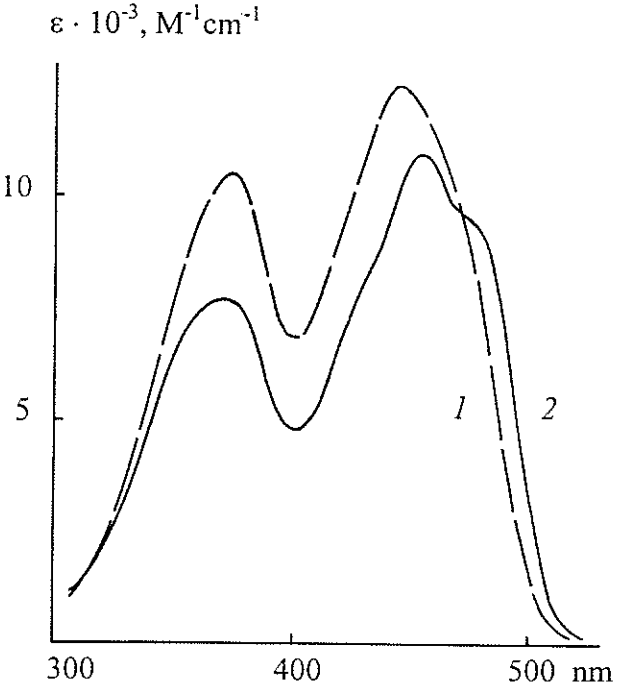

Figure 11.4. Spectra of free FMN (*1*) and FMN bound to muscle glycogen phosphorylase *b* (2) (Klinov *et al.*, 1986b).

Table 11.1. Changes in the spectral properties of riboflavin, FMN, and FAD induced by their binding to muscle glycogen phosphorylase *b*. 50 mM glycylglycine buffer, pH 6.8; 0.2 mM EDTA, 0.1 M KCl, 20°C (Klinov *et al.*, 1986b)

Flavin	Parameter	Free flavin		Bound flavin		
Riboflavin	λ_{max} (nm)	445	374	471*	451	371
	$\varepsilon \cdot 10^{-3}$ ($M^{-1}cm^{-1}$)	12.3	10.8	9.4*	10.9	7.9
FMN	λ_{max} (nm)	445	373	471*	453	371
	$\varepsilon \cdot 10^{-3}$ ($M^{-1}cm^{-1}$)	12.5	10.4	9.6*	11.0	7.7
FAD	λ_{max} (nm)	450	375	472*	452	371
	$\varepsilon \cdot 10^{-3}$ ($M^{-1}cm^{-1}$)	11.3	9.3	9.3*	10.8	7.7

* the shoulder

FMN is evaluated to be equal to 98% at the enzyme and flavin concentrations used (Klinov *et al.*, 1986b), as calculated using the known value of the microscopic dissociation constant for the complex between phosphorylase *b* and flavin (see below). Thus, it seems reasonable to suppose that the measured absorbance spectrum corresponds to that of protein-bound FMN. Riboflavin and flavin-adenine dinucleotide (FAD) revealed similar absorbance spectra both in the absence and in the presence of phosphorylase *b* (Klinov *et al.*, 1986b). The spectral characteristics for free and protein-bound flavins are summarized in *Table 11.1*. The binding of flavins to muscle phosphorylase *b* is accompanied by a decrease in the intensity of their first and second absorption bands. The maximum of the first absorption band is displaced towards higher wavelengths, the maximum of the second absorption band is displaced towards lower wavelengths and a markedly pronounced shoulder appears on the red side of the first absorption band (*Table 11.1*). The shoulder appearing in the spectrum of protein-bound flavin was at 471 nm in the case of riboflavin and FMN and at 472 nm in the case of FAD. The molar extinctions of protein-bound flavins are practically identical across the wavelength spectrum analysed. The total spectral characteristics for protein-bound flavins are practically the same (*Table 11.1*). This fact indicates that the environment of the isoalloxazine chromophore of riboflavin, FMN, and FAD is characterized by similar hydrophobicity in the complex between glycogen phosphorylase *b* and flavin (Klinov *et al.*, 1986b).

THE INHIBITION OF GLYCOGEN PHOSPHORYLASE *b* BY FLAVINS

The inhibition of phosphorylase *b* from rabbit skeletal muscles by flavins has been studied using the turbidimetric method for monitoring the enzymatic reaction rate (Klinov *et al.*, 1986a). The value of the initial steady-state rate for the reaction catalyzed by glycogen phosphorylase *b* is decreased in the presence of FMN or FAD (*Figure 11.5*). The inhibition is reversible, suggesting that the interaction between phosphorylase *b* and flavin is of a non-covalent character. The following linear anamorphosis of the Hill equation was used for the quantitative description of the dependence of the relative rate of the enzymic reaction on the flavin concentration (see Kurganov, 1982):

$$\ln (v_0/v_i - 1) = h \ln [I]_0 - h \ln [I]_{0.5}, \qquad (11.2)$$

where v_0 and v_i are the initial rates of the enzymatic reaction in the absence and in the presence of inhibitor respectively; $[I]_0$ is the total concentration of the inhibitor; $[I]_{0.5}$

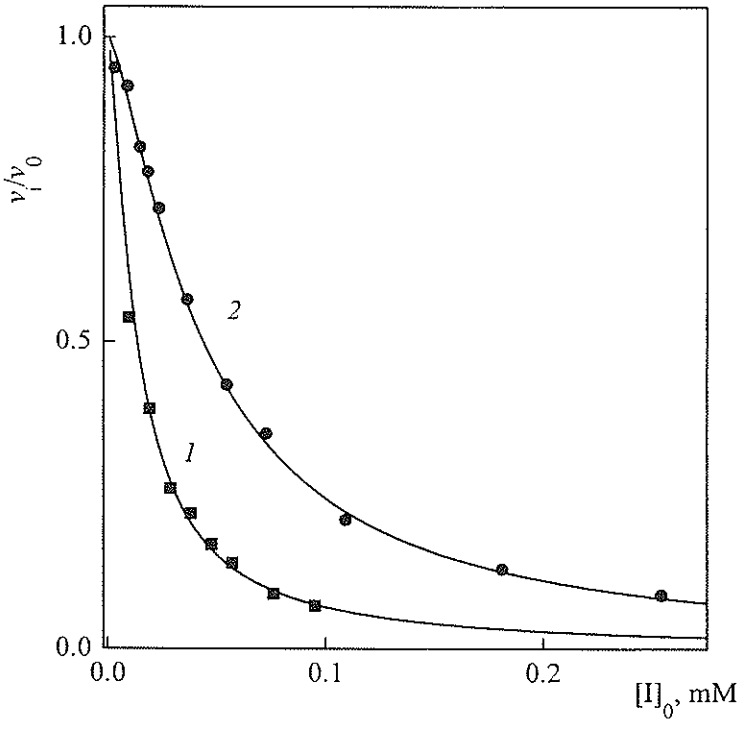

Figure 11.5. The dependence of the relative rate of glycogen synthesis catalyzed by muscle glycogen phosphorylase *b* in the presence of 0.1 mM AMP and 4 mM glucose-1-P on the concentration of the inhibitor: FMN (*1*) and FAD (*2*). 50 mM glycylglycine buffer, pH 6.8 containing 0.2 mM EDTA and 0.3 M KCl; 30°C (Klinov *et al.*, 1986a).

Table 11.2. The parameters of the Hill equation for the inhibition of muscle glycogen phosphorylase *b* by flavins. 50 mM glycylglycine buffer, pH 6.8; 0.2 mM EDTA, 0.3 M KCl, 30°C (Klinov *et al.*, 1986a)

Flavin	*h*	$[I]_{0.5}$, μM
Riboflavin	1.09 ± 0.03	18 ± 2
FMN	1.31 ± 0.04	13.5 ± 0.6
FAD	1.37 ± 0.02	43.8 ± 0.4

is the inhibitor concentration at which $v_i/v_0 = 1/2$; and *h* is the Hill coefficient. The values of the parameters of the Hill equation are shown in *Table 11.2*. The inhibitory action of flavins on phosphorylase *b* is characterized by positive kinetic cooperativity (the Hill coefficient exceeds unity). The chemical modification of the flavin molecule slightly changes the value of the Hill coefficient, but causes a marked increase in $[I]_{0.5}$, whose reciprocal value may be considered as a parameter characterizing the affinity of the enzyme for the inhibitor. The introduction of the bulky N-acetyl-L-cystein-S-yl radical in the position 8α of the isoalloxazine ring of the FMN molecule results in a 19-fold increase in the $[I]_{0.5}$ value, whereas the introduction of this radical in the

position 6 results in a less than 3-fold increase in the value of this parameter. The acetylation of all the hydroxy groups of the ribityl chain of riboflavin results in a 13-fold increase in the $[I]_{0.5}$ value. These facts demonstrate that the affinity of phosphorylase *b* to modified flavins depends on the chemical nature of the substituent and its position in the flavin molecule. The decreased affinity of the modified flavins to phosphorylase *b* seems to be due to a negative steric or/and electronic effect of the substituent on the binding of the ligand to the enzyme (Klinov and Kurganov, 1995).

SEDIMENTATION ANALYSIS OF BINDING OF FLAVINS BY PHOSPHORYLASE *b*

Binding of flavins to phosphorylase *b* was studied by the sedimentation velocity and equilibrium methods (Klinov *et al.*, 1984; Chebotareva *et al.*, 1986, 1991, 1995; Chebotareva, 1988; Eronina *et al.*, 1996) using a Model E (Beckman) analytical ultracentrifuge equipped with the scanning absorption optical system.

(i) Sedimentation velocity study

A typical sedimentation velocity pattern for the enzyme–flavin complex is shown in *Figure 11.6a* (Chebotareva *et al.*, 1986). Sedimentation was registered at the wavelength corresponding to the absorbance maximum of FMN (445 nm). The absorbance of the enzyme in this region was negligibly small. FMN does not sediment under selected conditions and therefore the sedimentation boundary observed corresponds to the moving of the enzyme–flavin complex. The plateau formed after the passage of the moving boundary is a measure of the free ligand concentration [L]. The concentration of a bound ligand [EL] was calculated as the difference between the total concentration of the ligand, $[L]_0$, and concentration of the free ligand [L]. In order to calculate the number of flavin-binding sites (n) and the microscopic dissociation constant (K_L) of the enzyme–FMN complex, the results of the FMN binding experiments were plotted according to the Scatchard equation:

$$\frac{r}{[L]} = \frac{n}{K_L} - \frac{1}{K_L}, \tag{11.3}$$

where r is moles of ligand bound per mole of enzyme monomer, n is the number of FMN-binding sites in the enzyme monomer. The values of K_L and n obtained from the Scatchard plot (*Figure 11.6b*) are 6.8 ± 0.5 μM and 0.96 ± 0.08 respectively (pH 6.8, 20°C), i.e. each enzyme subunit binds one FMN molecule. Thus, the sedimentation results are consistent with those of the X-ray study demonstrating the existence of one FMN-binding site per phosphorylase *a* monomer (Sprang *et al.*, 1982).

The sedimentation velocity method was used also for the study of riboflavin and FAD binding by phosphorylase *b* (Chebotareva *et al.*, 1986; Chebotareva, 1988). Analysis of the data was performed for the complex stoichiometry 1:1 using the equation:

$$[E] = K_L\,[EL]/[L], \tag{11.4}$$

where [E] is the concentration of the free enzyme. The microscopic dissociation constants for the complexes of the enzyme with riboflavin and FAD were found to be 12.5 ± 0.5 and 18.0 ± 0.7 μM respectively (0.1 M KCl, pH 6.8, 20°C).

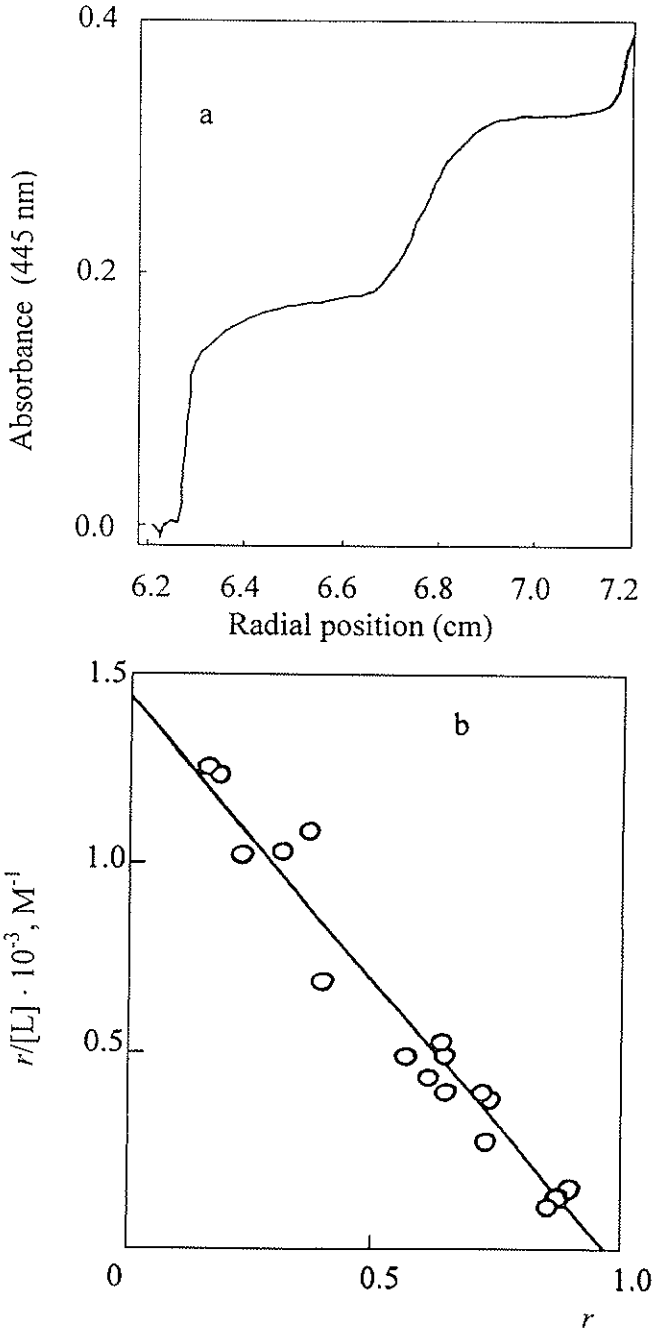

Figure 11.6. The binding of FMN by muscle phosphorylase *b*. 50 mM glycylglycine buffer, pH 6.8; 0.2 mM EDTA, 0.1 M KCl, 20°C. (a) Sedimentation velocity pattern of the enzyme–FMN complex. Rotor speed is 60,000 rev/min. Total concentration of the enzyme calculated on the monomer is 25 μM. Total concentration of FMN is 28 μM. (b) The Scatchard plot (Chebotareva *et al.*, 1986).

(ii) Interaction of FMN with apophosphorylase b

As was mentioned above, the catalytic site of each subunit of phosphorylase *b* contains one molecule of covalently bound coenzyme, pyridoxal-5'-phosphate (PLP). Removal of PLP results in the loss of the catalytic activity and dissociation of dimer to monomers (Gunar *et al.*, 1990; Helmreich, 1992). Reconstitution of phosphorylase *b* from apoenzyme and PLP is accompanied by the recovery of the catalytic activity and the quaternary structure of the enzyme (Hedrick *et al.*, 1966; Gunar *et al.*, 1990; Helmreich, 1992). Analysis of the data on binding of apophosphorylase *b* with FMN was performed using *Equation 11.4*. The dissociation constant for the complex FMN–apophosphorylase *b* was found to be $K_L = 240 \pm 23$ μM (Chebotareva *et al.*, 1995). The K_L value in the case of apophosphorylase *b* was significantly greater than the corresponding value for the native enzyme. Thus, the PLP molecule plays an important role not only in the catalytic function of phosphorylase *b*, but also in realization of inhibitory action of flavins, which occupy the nucleoside inhibitor site.

(iii) Sedimentation equilibrium study

In addition to the sedimentation velocity method, binding of FAD by phosphorylase *b* has been investigated using the sedimentation equilibrium method (Chebotareva *et al.*,

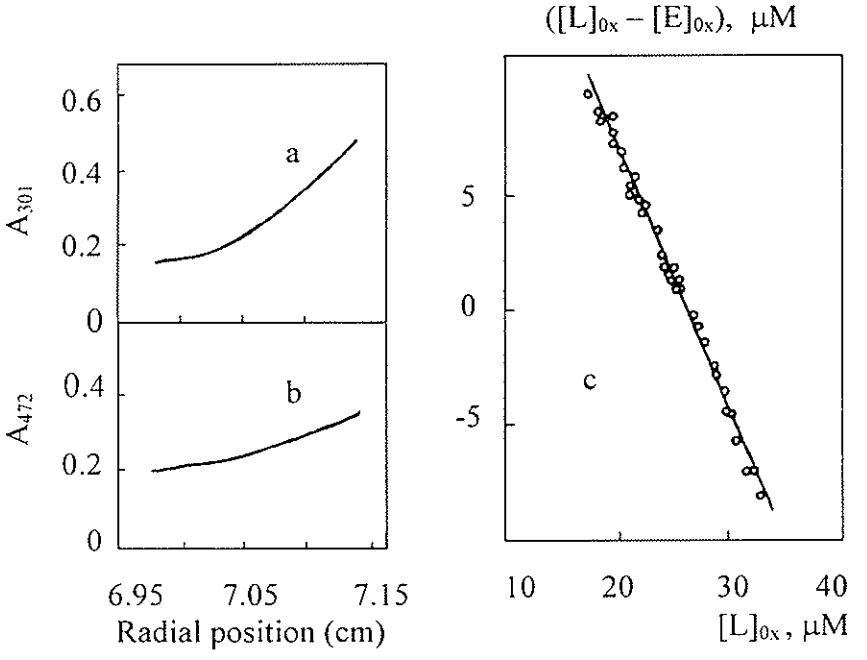

Figure 11.7. The binding of FAD by phosphorylase *b*. 50 mM glycylglycine buffer, pH 6.8; 0.2 mM EDTA, 0.1 M KCl, 20°C. Spinco, model E analytical ultracentrifuge equipped with scanning absorption optics was used. (a) Sedimentation equilibrium pattern for the enzyme. The wavelength of light is 301 nm. (b) Sedimentation equilibrium pattern for the enzyme–FAD mixture. The wavelength of incident light is 472 nm. Rotor speed is 9000 rev/min, duration of the experiment is 10 h at 20°C. The loading concentrations of the enzyme and FAD were 24.5 and 24.1 μM, respectively. (c) Linear anamorphosis of the data on FAD binding (*Equation 11.8*) (Chebotareva *et al.*, 1986).

1986). The rigorous theory of application of this method to the study of ligand–protein systems was elaborated by Steinberg and Schachman (1966). The method gives more reliable values for the dissociation constant of the enzyme–ligand complex, since no transport of the substance in the centrifugal field occurs at the sedimentation equilibrium. Besides, the relatively low rotor speed and, consequently, a low pressure gradient which may affect the state of the chemical equilibrium are used in this method. The equilibrium distributions of the enzyme and FAD in the presence of phosphorylase *b* are presented in *Figure 11.7a* and *11.7b* respectively. Only bound FAD is redistributed along the cell radius, whereas the concentration of the free ligand is constant. Absorbance of FAD (initial concentration 24.1 μM) in the presence of the enzyme (initial concentration 24.5 μM) was monitored at 472 nm (*Figure 11.7b*). At this wavelength the extinction coefficients for the free and bound ligand are identical ($\varepsilon_{472} = 0.93 \cdot 10^4\ M^{-1}cm^{-1}$). The enzyme does not absorb at 472 nm. The total concentrations of the ligand $[L]_{0x}$ and the enzyme $[E]_{0x}$ at the chosen radial distance, x, are expressed as concentrations of the bound ligand $[EL]_x$, free ligand [L], and free enzyme $[E]_x$:

$$[L]_{0x} = [L] + [EL]_x, \tag{11.5}$$

$$[E]_{0x} = [E]_x + [EL]_x. \tag{11.6}$$

The following relationship is true for [L], $[E]_x$ and $[EL]_x$ (if the complex stoichiometry is 1:1):

$$K_L = [L]\,[E]_x / [EL]_x. \tag{11.7}$$

To calculate the dissociation constant, K_L, the following anamorphosis was used:

$$[L]_{0x} - [E]_{0x} = (K_L + [L]) - (K_L/[L])[L]_{0x}. \tag{11.8}$$

The linear anamorphosis deduced on the basis of the experimental data is given in *Figure 11.7c*. The dissociation constant for the enzyme–FAD complex, K_L, is 18.1 ± 0.2 μM. Thus, both sedimentation velocity and equilibrium methods gave the coinciding values of K_L: 18.0 ± 0.7 and 18.1 ± 0.2 μM respectively.

The data on binding of flavins with phosphorylase *b* obtained by the different methods are summarized in *Table 11.3*. Comparing the experimental value of the dissociation constant for the FAD–enzyme complex (18.1 μM) with that for the FMN–enzyme complex (6.8 μM), one can conclude that the affinity of the enzyme to

Table 11.3. Microscopic dissociation constants (K_L) for the complexes of phosphorylase *b* with flavins (pH 6.8)

Flavin	K_L, μM (Temperature)	Method	Reference
Riboflavin	12.5 ± 0.5 (20°C)	Sedimentation velocity	Chebotareva *et al.* (1986)
Riboflavin	30 ± 1 (37°C)	Tryptic digestion	Kurganov *et al.* (1993)
FMN	6.8 ± 0.5 (20°C)	Sedimentation velocity	Chebotareva *et al.* (1986)
FMN	13.8 ± 0.8 (37°C)	Sedimentation velocity	Kurganov *et al.* (1993)
FMN	15.8 ± 0.2 (37°C)	Tryptic digestion	Kurganov *et al.* (1993)
FAD	18.0 ± 0.7 (20°C)	Sedimentation velocity	Chebotareva *et al.* (1986)
FAD	18.1 ± 0.2 (20°C)	Sedimentation equilibrium	Chebotareva *et al.* (1986)
FAD	25 ± 1 (37°C)	Sedimentation velocity	Eronina *et al.* (1992)
FAD	36 ± 1 (37°C)	Tryptic digestion	Kurganov *et al.* (1993)

the dinucleotide coenzyme form of vitamin B_2 is three times less than the affinity to the mononucleotide form. The affinity of the enzyme to FMN is almost two times more than that to riboflavin (*Table 11.3*). The possible explanation is that FAD, like NADH (Stura *et al.*, 1983), retains a folded conformation, when binding to the enzyme. The greater affinity of FMN in comparison with riboflavin is probably due to the formation of additional contacts between phosphate of FMN and amino acid residues of the protein molecule. It is worthwhile noting that the dissociation constants for FMN, riboflavin, and FAD correlate with the $[I]_{0.5}$ values characterizing the inhibiting capacity of flavins (*Table 11.2*).

ANALYSIS OF THE AFFINITY TO FLAVINS ON THE BASIS OF THE DATA ON PHOSPHORYLASE *b* TRYPSINOLYSIS

Hydrolysis of phosphorylase *b* by trypsin is accompanied by diminishing the intensity of protein fluorescence with batochromic shift of the emission maximum (*Figure 11.8*). Such changes in fluorescence of phosphorylase *b* are due to an increase in exposure of tryptophan residues of the enzyme molecule during trypsinolysis. *Figure 11.9* shows a diminishing relative intensity of phosphorylase *b* fluorescence (I/I_0) during hydrolysis by trypsin. The initial part of the kinetic curve is linear over at least 400 s (curve *1*). The initial rate of trypsinolysis registered by the change in the intensity of phosphorylase *b* fluorescence ($w = d(I/I_0)/dt$) decreases, when trypsin is added to phosphorylase *b* preincubated with FMN for 10 min. At 10 μM FMN a 1.7-fold decrease in the initial rate of trypsinolysis is observed (curve *2*).

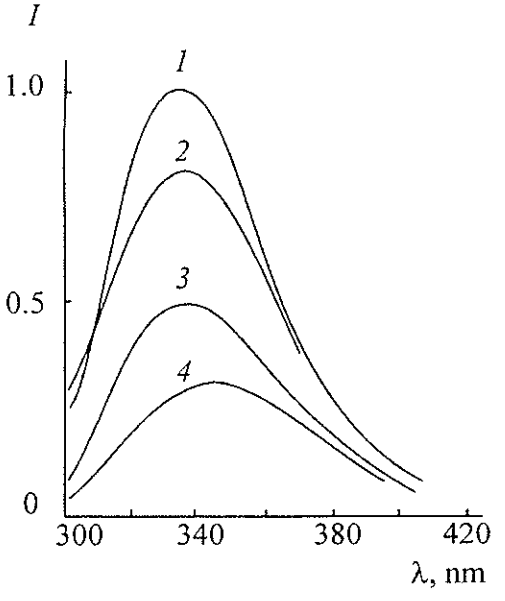

Figure 11.8. Changes in the fluorescence spectra of muscle phosphorylase *b* caused by trypsinolysis (excitation with the wavelength of 290 nm) (Kurganov *et al.*, 1994b). *I* is the intensity of fluorescence in arbitrary units. Time of hydrolysis (min): 0 (*1*); 2 (*2*); 5 (*3*), and 10 (*4*). Phosphorylase *b* 0.1 mg/ml, trypsin 0.067 mg/ml. 0.2 M Hepes, pH 6.8, 37°C.

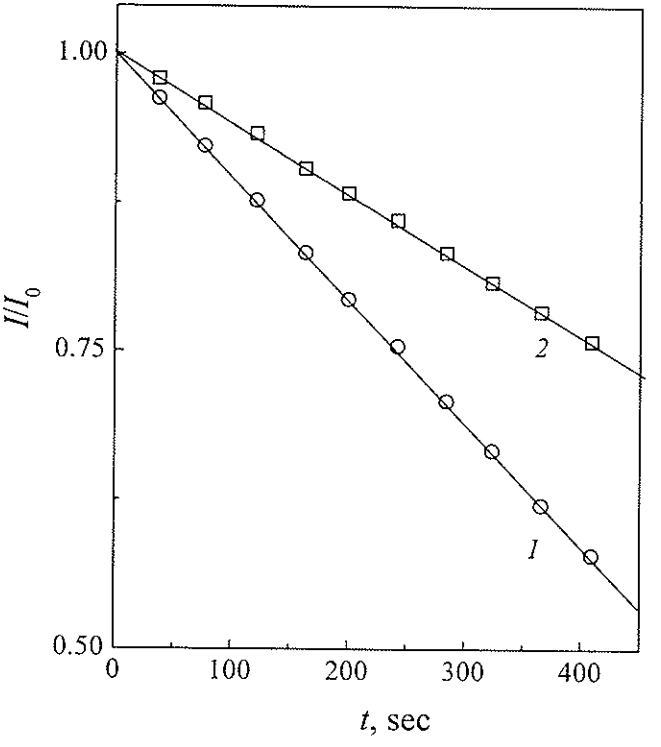

Figure 11.9. Influence of FMN on the kinetics of hydrolysis of phosphorylase *b* by trypsin (0.2 M Hepes, pH 6.8; 37°C) (Schors *et al.*, 1991). The time-course of the relative intensity of fluorescence (I/I_0) registered in the absence (*1*) or in the presence of 10 μM FMN (*2*).

The dependence of the initial rate of trypsinolysis on FMN concentration may be used for the estimation of the affinity of the enzyme to flavin. Assume that the protective action of FMN with respect to individual subunit in the dimeric molecule of phosphorylase *b* is the same, irrespective of whether the neighbouring subunit contains bound FMN. In this case the dependence of the initial rate of trypsinolysis on FMN concentration has the following form (Kurganov *et al.*, 1994b):

$$\frac{w_L}{w_0} = \frac{1 + \alpha[L]/K_L}{1 + [L]/K_L}, \qquad (11.9)$$

where w_0 and w_L are the initial rate of trypsinolysis in the absence and in the presence of FMN respectively, [L] is concentration of FMN, and α is the ratio of the initial rate of trypsinolysis for the enzyme saturated by FMN to w_0. *Figure 11.10* shows the dependence of w_L/w_0 on FMN concentration. Application of *Equation 11.9* for description of this dependence has given the following values of parameters: K_L = 15.8 ± 0.2 μM and α = 0.02 ± 0.02 (pH 6.8; 37°C). The fact that $\alpha \approx 0$ implies practically complete resistance of the FMN–phosphorylase *b* complex to trypsin attack (with the use of method of trypsinolysis registration based on diminishing the intensity of phosphorylase *b* fluorescence). The values of the microscopic dissociation constants for the complexes of phosphorylase *b* with FMN, FAD, and riboflavin estimated by the method described in this section are given in *Table 11.3*.

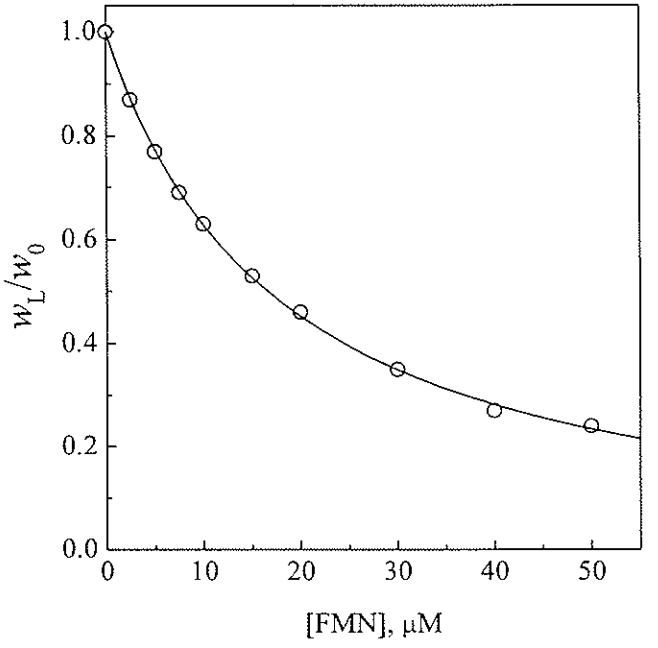

Figure 11.10. Protection of phosphorylase *b* from hydrolysis by trypsin in the presence of FMN (0.2 M Hepes, pH 6.8; 37°C) (Kurganov *et al.*, 1994b). The dependence of the relative rate of trypsinolysis w_L/w_0 measured from the decrease in the intensity of phosphorylase *b* fluorescence on FMN concentration. Points are experimental data. Solid curve is calculated from *Equation 11.9*.

Self-association of phosphorylase *b* induced by AMP

At neutral pH and low protein concentration phosphorylase *b* exists in the dimeric form. Conformational changes induced by AMP binding in the allosteric activatory site favour self-association of phosphorylase *b*. The position of dimer–tetramer equilibrium depends on the enzyme concentration, pH, ionic strength, temperature, and the presence of allosteric effectors and substrates. Sulphate ions and glucose-1-P favour the association, whereas the presence of glycogen and inhibitors (ATP, ADP, caffein, adenosin, adenin, flavins, NADH, glucose, and glucose 6-phosphate) prevent the formation of tetramers (Silonova and Lisovskaya, 1967; Silonova and Kurganov, 1970; Dombradi 1981; Munos *et al.*, 1983; Chebotareva *et al.*, 1986, 1991, 1995, 1998; Chebotareva, 1988; Klinov *et al.*, 1988; Klinova *et al.*, 1988).

(i) Sedimentation equilibrium study

Association of the phosphorylase *b* induced by 1 mM AMP in the presence of 0.125 M K_2SO_4 and 4 mM glucose-1-P has been investigated by the sedimentation equilibrium methods at 17°C in 50 mM glycylglycine buffer, pH 6.8, containing 0.2 mM EDTA (*Figure 11.11*) (Chebotareva *et al.*, 1998). The dimer–tetramer model provides an appropriate description of the reversible association of phosphorylase *b*. The molar association constant K_{ass} was found to be 1.5×10^6 M^{-1}.

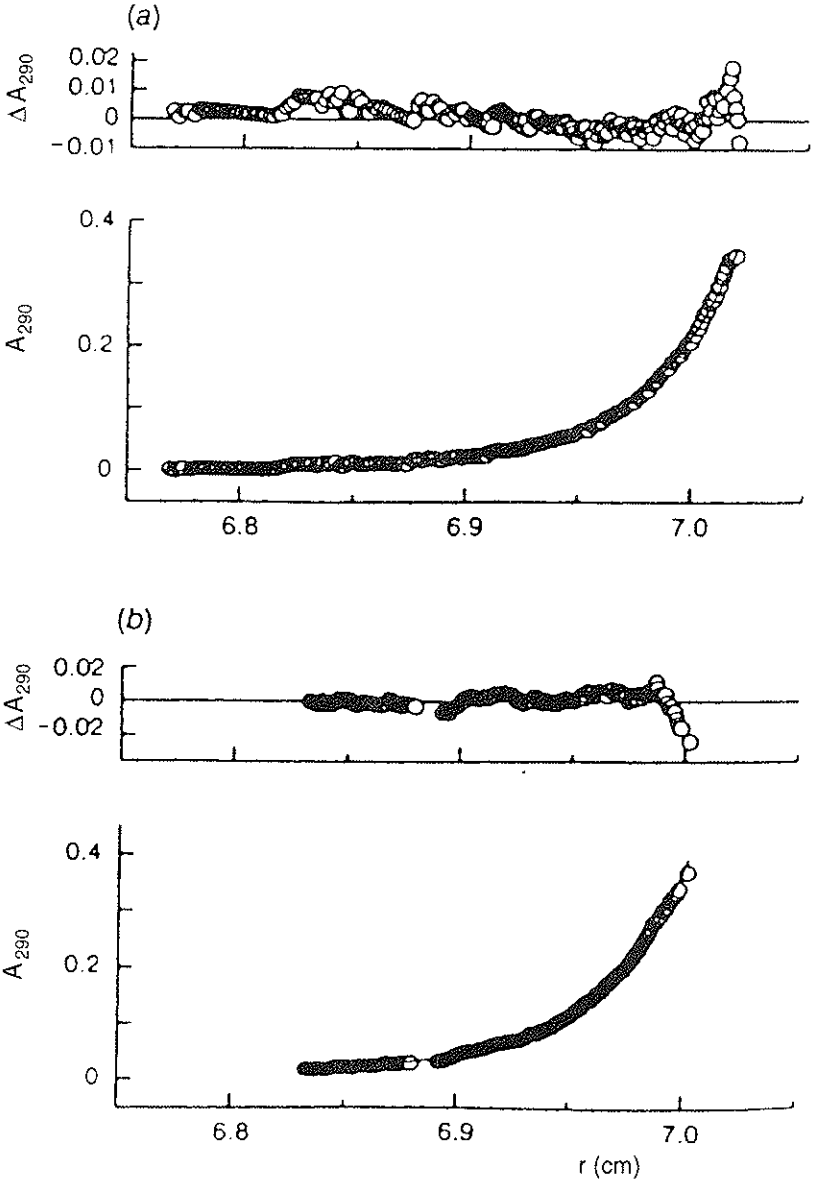

Figure 11.11. Concentration distribution and distribution of the residuals as functions of radial position for phosphorylase *b* at sedimentation and chemical equilibrium after 26 h at 10,000 rev/min. Spinco, Model E analytical ultracentrifuge equipped with scanning absorption optics was used. Overspeeding (15,000 rev/min, 3 h) was applied. Sedimentation was at 17°C in 0.05 M glycylglycine buffer, pH 6.8, containing 0.2 mM EDTA, 0.125 M K_2SO_4, 1 mM AMP, and 4 mM glucose-1-P. FC-43 oil was placed at the bottom of the cells. The fitting curve is calculated for a thermodynamically ideal homogeneous dimer–tetramer association of phosphorylase *b*. The loading concentration was 0.37 mg/ml (a) and 0.92 mg/ml (b) (Chebotareva *et al.*, 1998).

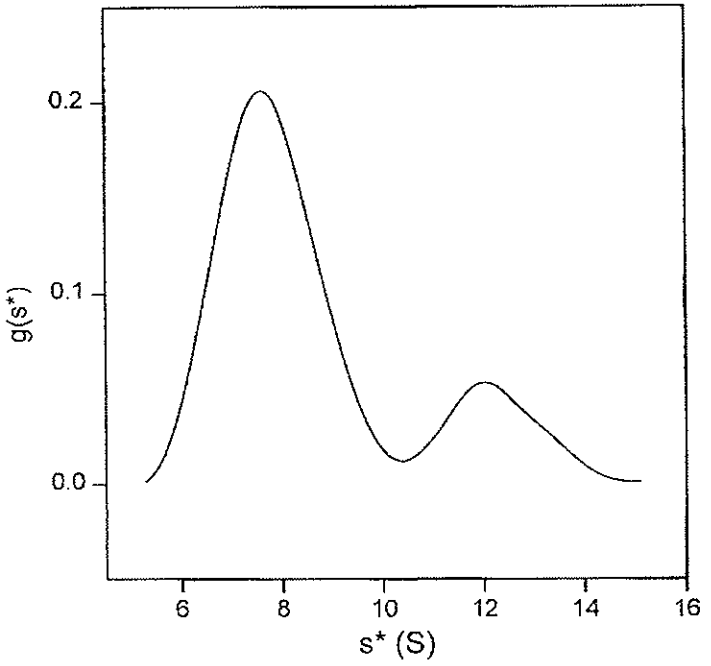

Figure 11.12. Sedimentation velocity behaviour of phosphorylase *b* in 40 mM Hepes (pH 6.8) in the presence of 1 mM AMP. Apparent sedimentation coefficient distribution, g(s*) versus s* (Chebotareva *et al.*, 2001), calculated by the method of Stafford (1992).

(ii) Sedimentation velocity analysis of self-association of phosphorylase b

Under certain conditions the dimer–tetramer interconversion is sufficiently slow to allow the separation of two species by sedimentation velocity (Sealock and Graves, 1967; Chebotareva, 1988; Chebotareva *et al.*, 1991, 1995, 2001; Eronina *et al.*, 1996). This aspect of the sedimentation velocity behaviour of phosphorylase *b* in an experiment conducted at 48,000 rpm is illustrated in *Figure 11.12* which comprises two clearly resolved g(s*) peaks, corresponding to the dimeric and tetrameric species (Chebotareva *et al.*, 2001). The association constant K_{ass} for dimer–tetramer equilibrium was calculated by equation (Chebotareva *et al.*, 1991):

$$K_{ass} = (1 - \gamma)/2\gamma^2[E]_0, \tag{11.10}$$

where γ is the portion of dimer, $[E]_0$ is the molar concentration of the enzyme per dimer. Interpretation of the areas of the two g(s*) peaks (*Figure 11.12*) in terms of *Equation 11.10* yields the association constant, K_{ass}, of 3.0×10^4 M^{-1} for phosphorylase *b* under given conditions (40 mM Hepes buffer, pH 6.8, containing 1 mM AMP; 15°C) – a value which is in reasonable agreement with that of 2.4×10^4 M^{-1} deduced previously by sedimentation velocity under similar, but not identical, conditions (50 mM glycylglycine buffer, pH 6.8, containing 0.1 M KCl, 1 mM AMP; 17°C).

THE EFFECT OF FLAVINS ON DIMER–TETRAMER EQUILIBRIUM

Chebotareva and co-workers (Chebotareva, 1988; Chebotareva *et al.*, 1991, 1995) have studied the flavin influence on the oligomeric state of phosphorylase *b* at 17°C under conditions of saturation of the allosteric activatory site by AMP (1 mM) and at high concentrations of the enzyme (6–8 mg/ml). Under such conditions both enzyme forms, dimeric and tetrameric, were present on the sedimentation patterns and the portion of the tetrameric form of the enzyme was significant (*Figure 11.13*) (Chebotareva *et al.*, 1991). Simultaneous use of the Schlieren and photoelectric

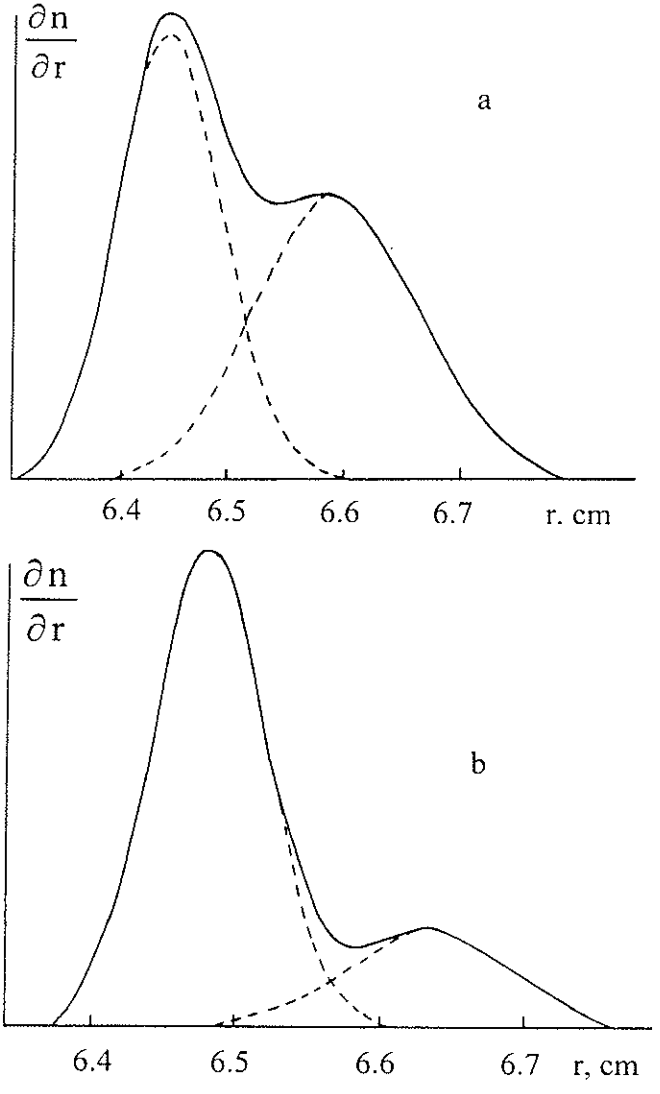

Figure 11.13. Schlieren patterns of phosphorylase *b* (7.6 mg/ml) in the absence (a) and in the presence of 72 μM FMN (b). Sedimentation was carried out for 30 min at 60,000 rev/min. r is the radial distance, ∂n/∂r is the refractive index gradient. 0.05 M glycylglycine buffer, pH 6.8 containing 0.1 M KCl and 1 mM AMP; 17°C (Chebotareva *et al.*, 1991).

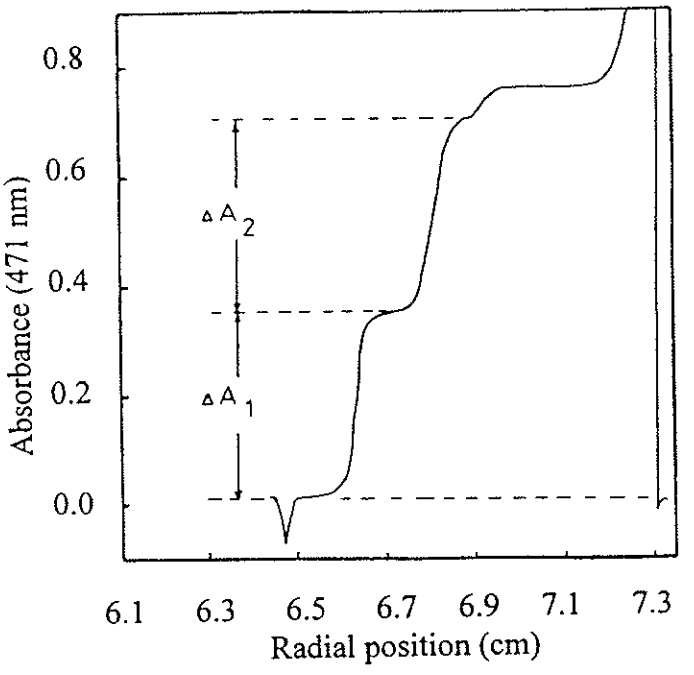

Figure 11.14. Sedimentation of the FMN–dimer and FMN–tetramer complexes, registered with absorption scanning optics. Conditions as in *Figure 11.13* (Chebotareva *et al.*, 1991).

scanning absorption optical systems of an analytical ultracentrifuge – the Spinco Model E – permits the oligomeric state of the enzyme to be registered and the degree of saturation of individual oligomeric forms by FMN to be calculated. Schlieren optics permit the enzyme oligomeric forms as two partially overlapping peaks to be recorded (*Figure 11.13*). To determine the amounts of FMN bound to the dimeric and tetrameric forms of phosphorylase *b* and the concentration of free FMN, the absorption optical system was used (*Figure 11.14*). The chosen wavelength (471 nm) corresponds to the isobestic point for absorption spectra of free and enzyme-bound FMN (Klinov *et al.*, 1986b). The rapidly moving boundary corresponds to sedimentation of the FMN–tetramer complex, whereas the slowly moving boundary characterizes sedimentation of the FMN–dimer complex. The plateau height (ΔA_1) formed near the meniscus after precipitation of the enzyme–ligand complex is in line with the optical density of free FMN and the concentration of free ligand [L] can be calculated as follows: $[L] = [L]_0 \Delta A_1 / A_0$, where $[L]_0$ is the total concentration of FMN, A_0 is the absorbance of the original FMN solution which is obtained independently. In a similar way, the concentration of the ligand bound to the dimeric form of the enzyme can be calculated from the height of the slowly moving boundary (ΔA_2): $[L]^D = [L]_0 \Delta A_2 / A_0$. The concentration of FMN bound to tetramer was calculated as follows: $[L]^T = [L]_0 - [L]^D - [L]$. The method proposed permits the dependence of the apparent association constant K_{ass} on the concentration of free FMN (*Figure 11.15*) and functions of saturation of the dimeric and tetrameric forms of phosphorylase *b* to be constructed (*Figure 11.16*) (Chebotareva *et al.*, 1991). The degree of saturation of the dimeric form with FMN was determined as the ratio of concentration of dimer-

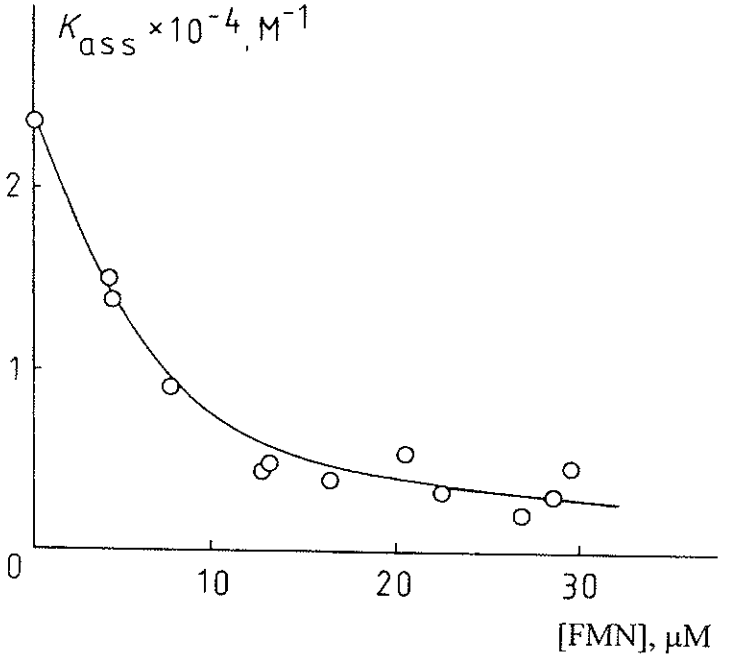

Figure 11.15. Dependence of the apparent association constant K_{ass} for the dimer–tetramer equilibrium on concentration of free FMN (in the presence of 1 mM AMP) (Chebotareva *et al.*, 1991).

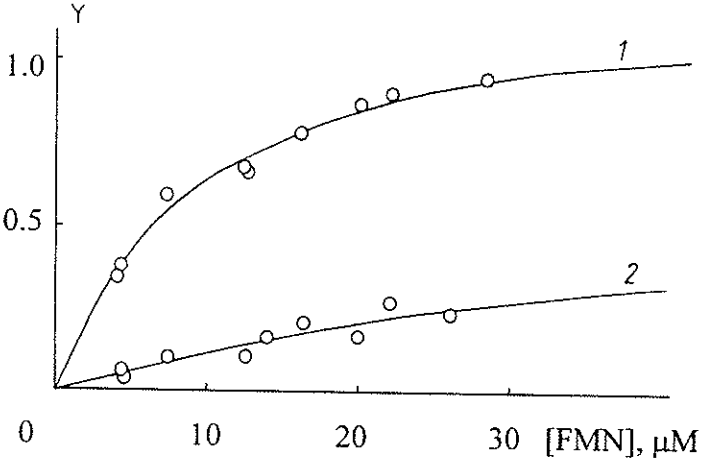

Figure 11.16. Function of saturation of dimeric (*1*) and tetrameric (*2*) forms of phosphorylase *b* with FMN. Conditions as in *Figure 11.13* (Chebotareva *et al.*, 1991).

bound FMN (a value estimated by means of absorption optics) to the molar concentration of dimer calculated on monomer (Chebotareva *et al.*, 1991) (a value estimated by means of Schlieren optics). In a similar way, the degree of saturation of tetramer with FMN was calculated. *Figure 11.16* shows the dependencies of the degree of saturation (Y) of dimer (*1*) and tetramer (*2*) with FMN on free FMN concentration.

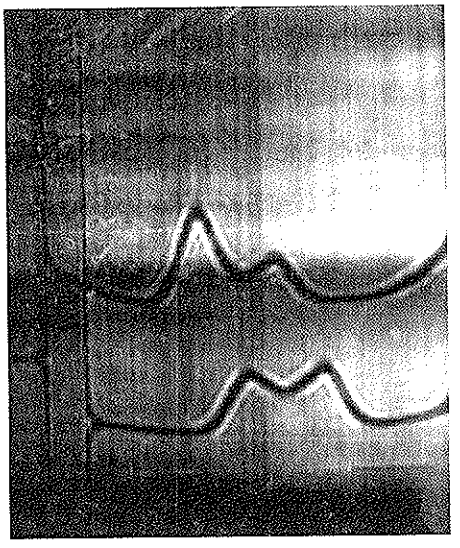

Figure 11.17. Sedimentation velocity patterns of phosphorylase *b* in the presence of 1 mM AMP (lower pattern, the portion of tetramer is 55%) and 10 mM AMP (upper pattern, the portion of tetramer is 30%) (Chebotareva, 1988). 50 mM glycylglycine buffer, pH 6.8; 0.1 M KCl, 18°C. The enzyme concentration is 7.3 mg/ml. Rotor speed is 56,000 rev/min.

The saturation functions were quantitatively treated assuming that ligand-binding sites of each oligomeric form are equivalent and non-interacting. The dependencies of saturation for dimer (*1*) and tetramer (*2*) with ligand (L) on free ligand concentration have a hyperbolic shape. The values of the dissociation constants for the complexes of the dimeric and tetrameric forms of phosphorylase *b* and FMN were found to be 10 $\pm$ 0.5 and 79 $\pm$ 8 μM, respectively. The K_L values obtained characterize the affinity of the oligomeric forms of phosphorylase *b* to FMN under the conditions of saturation of allosteric effector site by AMP.

It is interesting to note that AMP at relatively high concentration displaces dimer–tetramer equilibrium towards the dimeric form (*Figure 11.17*) (Chebotareva, 1988). The increase in AMP concentration from 1 mM to 10 mM results in 3–5-fold decrease in the K_{ass} value (Munos *et al.*, 1983; Chebotareva, 1988). According to data from microcalorimetry, equilibrium dialysis, and X-ray analysis (Wang *et al.*, 1970; Ho and Wang, 1973; Merino *et al.*, 1980; Munos *et al.*, 1983; Matco *et al.*, 1984), when used at high concentrations, AMP binds at the second allosteric site (inhibitory site) with a lower affinity. Thus, binding of AMP at the inhibitory allosteric site results in the weakening of bonds between dimers in the tetrameric form. This action of AMP is completely analogous to that of flavins.

The fact that allosteric activator AMP (at relatively low concentrations) favours self-association of phosphorylase *b*, whereas ligands binding at the allosteric inhibitory site (flavins, AMP at relatively high concentrations) favours the opposite effect, allows us to consider the tendency for association as a test for the changes in the conformation of the enzyme molecule induced by allosteric effectors.

Intramolecular dynamics of phosphorylase *b* registered by tryptophan phosphorescence

The problem of correlation between structure and functional activity of proteins is one of the most important problems in modern biology. There is a large body of experimental evidence for the functional significance of small- and medium-scale equilibrium intramolecular dynamics of protein structure. The characteristic time of the molecular dynamics ranges from 10^{-12} to 10^{-7} s (Mazhul *et al.*, 1970). Mechanisms of much slower Brownian motion of large polypeptide fragments, domains, and subunits are as yet insufficiently understood (Demchenko, 1988). The method of room temperature tryptophan phosphorescence (RTTP) is among a limited number of physical methods capable of providing information about the large-scale intramolecular dynamics of proteins. The tryptophan residue is widely used as an intrinsic phosphorescence probe to investigate the protein conformation and the structural changes. The lifetime (τ) and quantum yield (B) of the tryptophan phosphorescence are extraordinarily sensitive to changes in the molecular mobility in the chromophore proximity. This provides a unique opportunity for studying the protein intramolecular dynamics in a very broad range commensurate with the lifetime of the excited triplet state of tryptophan (10^{-6} to 10 s). If there is an increase in the experimentally observed values of τ and B, this corresponds to damping the low-frequency high-amplitude fluctuations of the protein structure, whereas a decrease in these parameters of tryptophan phosphorescence indicated activation of the large-scale intramolecular dynamics of proteins (Mazhul *et al.*, 1983, 1994; Strambini, 1989; Vanderkoi and Berger, 1989; Gonneli and Strambini, 1995).

Phosphorylase *b* is one of a few enzymes revealing millisecond RTTP in solution (Szarka *et al.*, 1998; Mazhul *et al.*, 1999). The spectrum of RTTP has a shoulder at 413 nm and maxima at 438 and 461 nm (*Figure 11.18*). A typical curve of the phosphorylase *b* phosphorescence decay kinetics can be adequately fitted by a sum of two exponential components (*Figure 11.19*). The lifetime values for the fast and slow components of phosphorescence at 20°C are $\tau_1 = 16.6 \pm 1.1$ ms and $\tau_2 = 72 \pm 10$ ms, respectively. The relative contribution of the fast component to the total phosphorescence decay curve under these conditions is $\alpha_1 = 0.48 \pm 0.09$. The phosphorylase *b* phosphorescence decay curves have been presented by Szarka *et al.* (1998) as sums of three exponential components. However, the relative amplitude of the third (slowest) component τ_3 was low (2–5%) and comparable with the measurement error.

It is well known that at room temperature the phosphorescence with $\tau > 1$ ms is inherent in tryptophanyl residues located in macromolecule domains with limited (hindered) intramolecular dynamics. The τ values of tryptophanyl residues located in the rigid hydrophobic core are significantly longer than the lifetime of chromophores located in the peripheral regions of the protein globule (Mazhul *et al.*, 1983, 1994; Strambini, 1989; Vanderkoi and Berger, 1989; Gonneli and Strambini, 1995). Because the phosphorylase *b* phosphorescence decay kinetics deviates from single exponential behaviour, the structural-dynamic properties of the macromolecule are thought to be heterogeneous. On the basis of the analysis of the spatial structure of the phosphorylase *b* molecule described by Acharya *et al.* (1991), it is believed that at room temperature the phosphorescence lifetime of two tryptophanyl

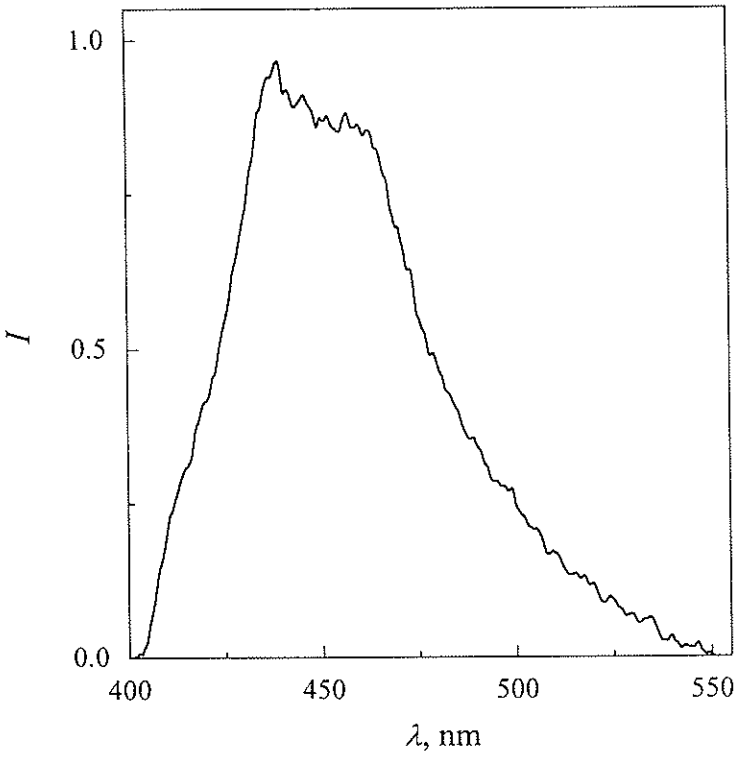

Figure 11.18. Spectrum of tryptophan phosphorescence of phosphorylase *b* (0.6 mg/ml) measured in 50 mM glycylglycine buffer, pH 6.8, at 20°C and corrected for the spectral sensitivity of the phosphorimeter (Mazhul *et al.*, 1999). Ordinate is the phosphorescence intensity (*I*) in arbitrary units.

residues deeply immersed in the protein globule interior (Trp244 and Trp491) is close to τ_2. Each of tryptophanyl residues located near the peripheral regions of the macromolecule (Trp67, Trp215, Trp361, Trp387, Trp797, and Trp285) may be responsible for the fast component of RTTP (τ_1), whereas Trp174 and Trp365 located on the surface of the phosphorylase *b* molecule presumably are not capable of emitting phosphorescence.

It was of special interest to study the effect of the substrate glucose-1-P on the molecular dynamics of phosphorylase *b*. Data obtained by Mazhul *et al.* (1999) has shown that binding of glucose-1-P to phosphorylase *b* induces an increase in the values of τ_1 and τ_2 (*Figure 11.20*). This increase is thought to be caused by inhibition of low-frequency high-amplitude fluctuations of the protein structure. The concentration dependences of the relative values of lifetimes $\tau_1/(\tau_1)_0$ and $\tau_2/(\tau_2)_0$ ($(\tau_1)_0$ and $(\tau_2)_0$ are the corresponding values of lifetimes in the absence of glucose-1-P) are S-shaped. This implies sufficiently strong positive cooperative interactions between the active sites in the dimeric enzyme molecule. The Hill coefficient is rather high ($h \cong 2$). It is believed that the restriction of low-frequency fluctuations of the phosphorylase *b* molecule induced by glucose-1-P may be due to cooperative interactions of subunits. It is significant that the results for the intramolecular dynamics of phosphorylase *b* registered by RTTP are consistent with the kinetic data demonstrating the positive

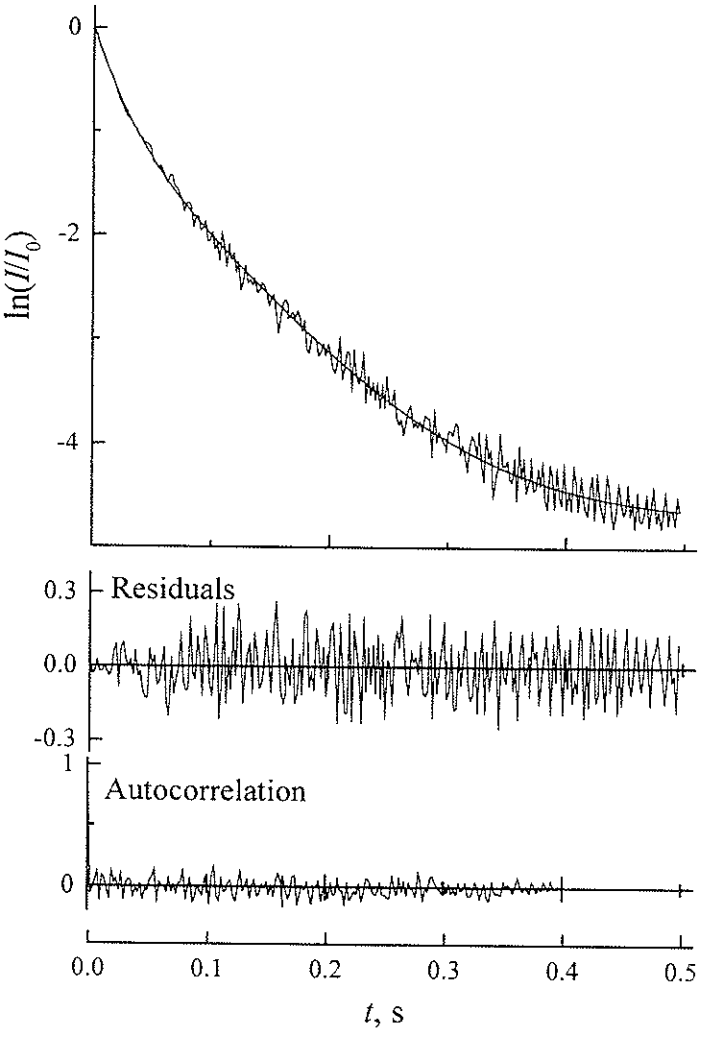

Figure 11.19. Kinetics of tryptophan phosphorescence decay of phosphorylase *b* (0.6 mg/ml) in 50 mM glycylglycine buffer, pH 6.8, at 20°C, distribution of weighted residuals, and residual autocorrelation function (Mazhul *et al.*, 1999).

kinetic cooperativity with respect to glucose-1-P (S-shaped dependencies of the enzymatic reaction rate on the substrate concentration).

The allosteric activator AMP, having the recognition site at the area of contact between the subunits, has no effect on the intramolecular dynamics of phosphorylase *b* registered by RTTP (Szarka *et al.*, 1998; Mazhul *et al.*, 1999). However, the enzyme association induced by AMP results in marked changes in the RTTP parameters. As can be seen from *Figure 11.21*, at rather high concentration of phosphorylase *b* a decrease in lifetime of tryptophan phosphorescence τ_1 is observed (the enzyme concentration was varied from 0.125 to 6.7 mg/ml). Apart from AMP, the incubation mixture contained K_2SO_4, which also favours the formation of tetramers. The

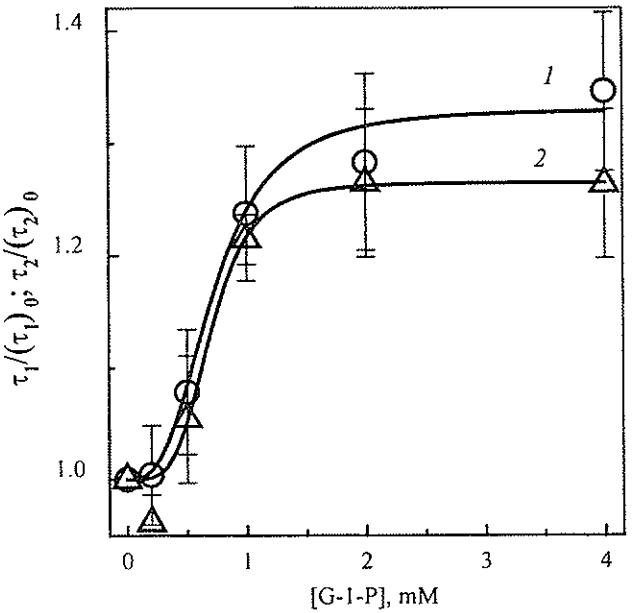

Figure 11.20. Dependence of the relative values of $\tau_1/(\tau_1)_0$ (*1*) and $\tau_2/(\tau_2)_0$ (*2*) for tryptophan phosphorescence of phosphorylase *b* (0.6 mg/ml) on the concentration of glucose-1-P in 50 mM glycylglycine buffer, pH 6.8, at 20°C (Mazhul *et al.*, 1999).

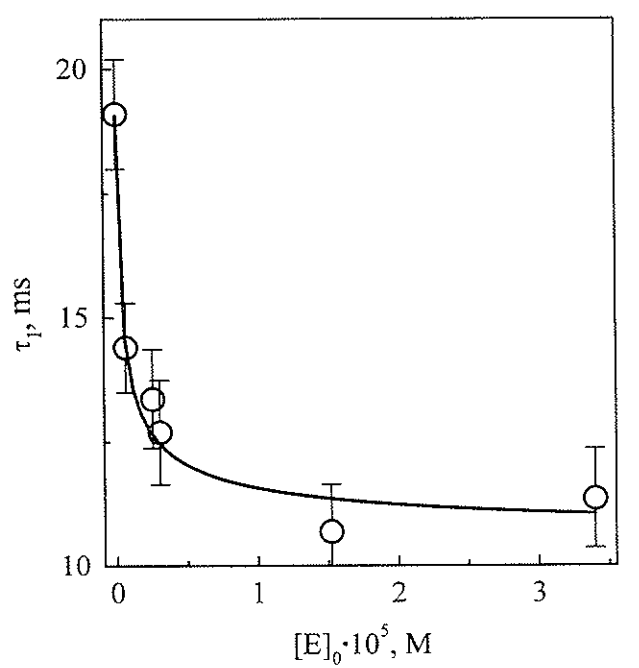

Figure 11.21. The dependence of the value of τ_1 for tryptophan phosphorescence of phosphorylase *b* on the molar enzyme concentration (per dimer) in 50 mM glycylglycine buffer, pH 6.8, containing 125 mM K_2SO_4, 1 mM AMP, and 4 mM glucose-1-P at 17°C (Mazhul *et al.*, 1999).

association constant for dimer–tetramer equilibrium calculated from the RTTP data was found to be $(3.9 \pm 0.6) \cdot 10^5$ M^{-1} (50 mM glycylglycine buffer, pH 6.8, containing 125 mM K_2SO_4, 1 mM AMP, and 4 mM glucose-1-P at 17°C) (Kurganov *et al.*, 1999). Thus, association of phosphorylase *b* dimers into tetramers is accompanied by an increase in the millisecond intramolecular dynamics of the protein structure. The mechanism of this effect is quite obscure. Probably, the effect is due to the conformational changes in the enzyme subunits caused by the interaction of dimers in the tetrameric enzyme molecule.

Influence of deimination on the catalytic properties and dimer–tetramer transition of phosphorylase *b*

Deimination of phosphorylase *b* by peptidylarginine deiminase has a pronounced effect on the binding of some allosteric effectors with the enzyme. The affinity of the modified phosphorylase *b* for the allosteric activator AMP is one order of magnitude higher than that of the native enzyme. Deimination has been found to cause a pronounced reduction of the values of $[I]_{0.5}$ for FMN and glucose, but the sensitivity of the deiminated enzyme to glucose 6-phosphate is much lower than that of the native phosphorylase *b* (Eronina *et al.*, 1996).

(i) The binding of FMN by deiminated phosphorylase b

Deiminated phosphorylase *b*, unlike the native enzyme, shows the positive cooperativity for FMN binding (*Figure 11.22*) (Eronina *et al.*, 1996). The sedimentation velocity method has been used to compare the binding of FMN by both forms of the enzyme. *Figure 11.22* presents the binding of FMN by the native (*1*) and deiminated (*2*) phosphorylase *b*. *Figure 11.22a* shows the saturation functions for the native and deiminated phosphorylase *b* for flavin binding, i.e. the dependencies of the degree of saturation r ($r = [EL]/[E]_0$, where $[E]_0$ is the total enzyme concentration calculated on monomer) on the equilibrium concentration of the ligand [L]. For the native enzyme the saturation function is hyperbolic (curve *1*): $r = [L]/(K + [L])$. It is interesting that the dependence of r on [L] for deiminated phosphorylase *b* is S-shaped, thus providing evidence of positive cooperative interactions between FMN-binding sites in the dimeric molecule of phosphorylase *b* (curve *2*; $h = 1.37 \pm 0.05$). The appearance of the saturation function for the deiminated enzyme in the coordinates $\{r;\ r/[L]\}$, corresponding to the Scatchard equation, supports the existence of positive cooperative interactions between flavin-binding sites in the molecule of the modified phosphorylase *b* (curve *2* in *Figure 11.22b*).

(ii) Association of the native and deiminated enzymes induced by AMP

Deiminated phosphorylase *b* shows less capability of forming tetramers in the presence of AMP as compared to the native enzyme. The association of dimers of the native phosphorylase *b* into tetramers induced by the allosteric activator is presented in *Figure 11.23*. Under the conditions used (1 mM AMP, 0.05 M glycylglycine buffer, pH 6.8, 17°C) phosphorylase *b* (7.6 mg/ml) sediments as two partially overlapping peaks (upper pattern) corresponding to the tetrameric form ($s_{20,w} = 12.0$ S) and dimeric

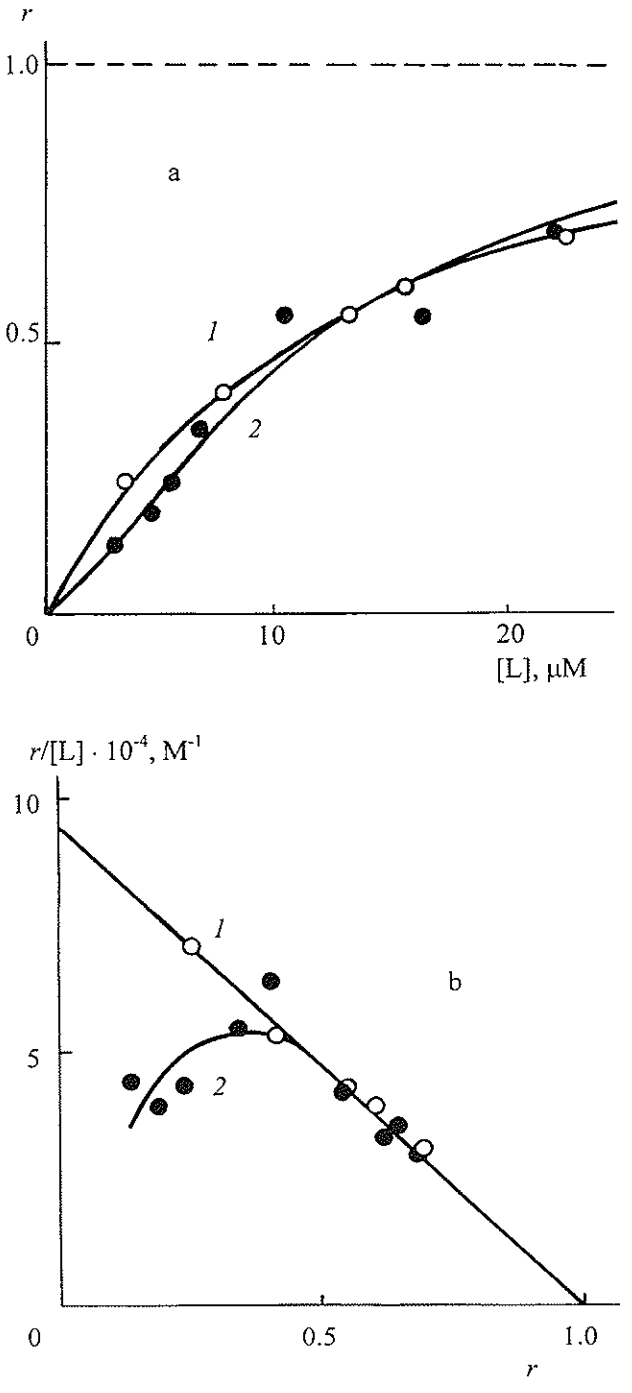

Figure 11.22. The binding of FMN by the native (*1*) and deiminated (*2*) phosphorylase *b*. 50 mM glycylglycine buffer, pH 6.8, 0.1 M KCl, 20°C. (a) The saturation function. (b) The Scatchard plot (Eronina *et al.*, 1996).

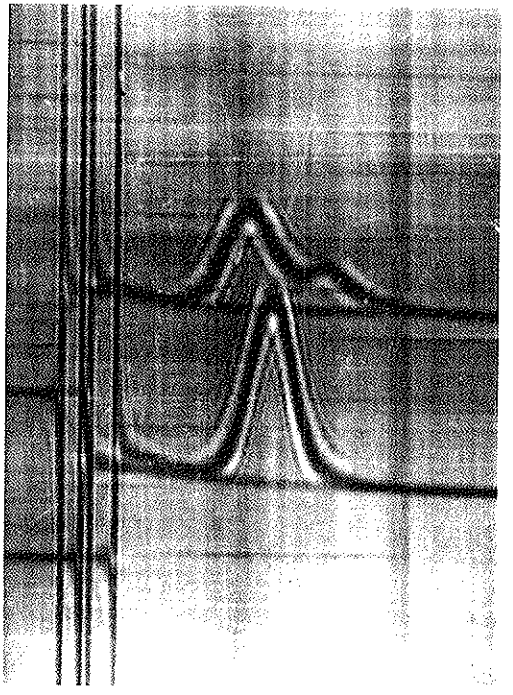

Figure 11.23. Sedimentation velocity patterns of the native (upper pattern) and deiminated (lower pattern) phosphorylase *b* in the presence of 1 mM AMP (Eronina *et al.*, 1996). 50 mM glycylglycine buffer, pH 6.8; 0.1 M KCl, 17°C. The enzyme concentration is 7.6 mg/ml. Rotor speed was 56,000 rev/min.

form ($s_{20,w} = 8.2$ S). The resolution of the upper curve into two components allows the portions of the dimeric and tetrameric forms and the association constant to be estimated: $K_{ass} = (2.4 \pm 0.4) \times 10^4 M^{-1}$. The lower pattern in *Figure 11.23* corresponds to the deiminated enzyme which sediments exclusively as a dimer. Thus, deimination of phosphorylase *b* considerably weakens the enzyme's capability to associate into tetramers in the presence of AMP. The influence of deimination of Arg16 on the dimer–tetramer transition in phosphorylase *b* is probably mediated by the conformational changes of the protein molecule, because direct participation in the tetramer formation was shown only for Arg724, Arg426, Arg569, and Arg770 (Barford and Johnson, 1992).

Concluding remarks

At the present time, considerable advances have been made in deciphering the spatial structure of the phosphorylase *b* molecule and the mechanisms of regulation of the enzyme activity by physiological effectors (cellular metabolites): these effectors include glucose-1-P (substrate), AMP (allosteric activator), flavins, adenosine, and other heterocyclic compounds (allosteric inhibitors). The allosteric activator and allosteric inhibitors have distinct binding sites and the interactions between the active and allosteric sites are mediated by conformational changes in the enzyme molecule (allosteric mechanism of regulation of enzyme activity). Furthermore, homotropic

allosteric interactions between the sites of the same type (for example, between glucose-1-P-binding sites, AMP-binding sites, or flavin-binding sites) are known to take place.

The changes in the conformation of phosphorylase *b* molecule accompanying the transition of the enzyme from the inactive form to the active one induced by ammonium sulphate have been characterized in detail by the X-ray method (Barford and Johnson, 1989). The binding of sulphate occurs at the catalytic site, the allosteric effector site, and Ser-phosphate site. The changes in the quaternary and ternary structures have been recorded. Each subunit rotates by 10° around an axis perpendicular to the symmetry axis of the second order of the dimeric enzyme molecule. The antiparallel association of the tower helices (the residues 262–276) possessed by both subunits is distorted. The tower helices in the activated form protrude from the main body of the enzyme. Movement of the tower helix indirectly leads to a replacement of Asp283 by Arg569 at the catalytic site, and the opening of tunnel to allow access for substrate.

On the basis of the kinetic analysis of the allosteric activation of phosphorylase *b* by AMP the conclusion has been made that only the complex of the dimeric enzyme molecule containing two AMP molecules occupying both allosteric effector sites, two molecules of glucose-1-P in both catalytic sites, and glycogen possess the catalytically active conformation.

What is the physiological function of binding of flavins by muscle phosphorylase? High affinity of phosphorylase to flavins suggests that the latter are capable of regulating the rate of glycogenolysis. In any case, by taking account of the high content of phosphorylase in skeletal muscles, it is believed that the enzyme may act as a depot of flavins. It is known also that glycogen synthase (EC 2.4.1.11) interacts with flavins, the latter inhibiting the enzyme activity (Solovyeva *et al.*, 1991). Phosphorylase and glycogen synthase, apart from other enzymes of glycogen metabolism (phosphorylase kinase, phosphorylase phosphatase, etc.), are the components of protein–glycogen particles in the muscle cells (Haschke *et al.*, 1970; Heilmeyer *et al.*, 1970; Meyer *et al.*, 1970). Thus, it is precisely the protein–glycogen particles that play the role of 'flavin depot'.

The conformational changes in the phosphorylase *b* molecule induced by allosteric activator AMP have been revealed in the enhanced ability of the enzyme to self-associate. Such an association on its own is not probably of physiological significance, because *in vivo* the greater part of phosphorylase is incorporated into the protein–glycogen particles. It is known that glycogen induces the dissociation of the tetrameric form of phosphorylase into dimers (Metzger *et al.*, 1967). Therefore, the presence of tetramers of phosphorylase *in vivo* is highly improbable. Nevertheless, when studying the enzymatic properties of phosphorylase *b in vitro*, the self-association may be considered as a test for the conformational changes in the enzyme molecule induced by binding of allosteric ligands (for example, allosteric inhibitors), enzymatic deimination, or replacement of PLP by its analogues (Chebotareva *et al.*, 1995).

The method of tryptophan phosphorescence at room temperature is promising in the study of the role of slow movements of the structural elements of the protein molecule in enzyme catalysis and its regulation. Application of this method to phosphorylase *b* has allowed the damping of the large-scale fluctuations of the enzyme molecule in the presence of the substrate glucose-1-P to be registered.

To summarize, it is evident that the combined use of the kinetic and physical methods will provide a deeper insight into the mechanisms of the catalytic action and regulation of phosphorylase.

Acknowledgement

This study was funded by grants 99-04-48639 and 00-15-97787 from the Russian Foundation of Basic Research.

References

ACHARYA, K.R., STUART, D.I., VARVILL, K.M. AND JOHNSON, L.N. (1991). *Glycogen phosphorylase b: Description of the protein structure,* pp 67–72. Singapore: World Scientific Publishing.

BARFORD, D. AND JOHNSON, L.N. (1989). The allosteric transition of glycogen phosphorylase *b*. *Nature* **340**, 609–616.

BARFORD, D. AND JOHNSON, L.N. (1992). The molecular mechanism for the tetrameric association of glycogen phosphorylase promoted by protein phosphorylation. *Protein Science* **1**, 472–493.

BARTFAI, T. AND MANNERVIK, B. (1972). A procedure based on statistical criteria for discrimination between steady state kinetic models. *FEBS Letters* **26**, 252–256.

BLACK, W.J. AND WANG, J.H. (1968). Studies on the allosteric activation of glycogen phosphorylase *b* by nucleotides. I. Activation of phosphorylase *b* by inosine monophosphate. *Journal of Biological Chemistry* **243**, 5892–5898.

BRESLER, S. AND FIRSOV, L. (1971). Allosteric interactions in phosphorylase *b*. *Biopolymers* **10**, 1187–1205.

BUC, M.H. AND BUC, H. (1968). Allosteric interactions between AMP and orthophosphate sites on phosphorylase *b* from rabbit muscle. In: *The Regulation of enzyme activity and allosteric interactions.* Eds. E. Kvamme and A. Pihl, pp 109–130. Oslo: Universitetsforlaget.

CHEBOTAREVA, N.A. (1988). Sedimentation analysis of allosteric, associative, and adsorptive enzyme systems. Thesis. Institute of Chemical Physics, Russian Academy of Sciences. Moscow.

CHEBOTAREVA, N.A., KURGANOV, B.I., PEKEL, N.D. AND BEREZOVSKII, V.M. (1986). Binding of vitamin B_2 and its coenzyme forms by muscle glycogen phosphorylase *b*. *Biochemistry International* **13**, 189–197.

CHEBOTAREVA, N.A., KURGANOV, B.I., LYUBAREV, A.E., DAVYDOV, D.R. AND PEKEL, N.D. (1991). Interaction of flavin mononucleotide with dimeric and tetrameric forms of muscle phosphorylase *b*. *Biochimie* **73**, 1339–1343.

CHEBOTAREVA, N.A., SUGROBOVA, N.P., BULANOVA, L.N., POZNANSKAYA, A.A., KURGANOV, B.I. AND GUNAR, V.I. (1995). Reconstitution of muscle glycogen phosphorylase *b* from apoenzyme and pyridoxal-5'-phosphate or its analogs. Interaction of apophosphorylase and the reconstituted enzyme with specific ligands. *Biochemistry (Moscow)* **60**, 1551–1558.

CHEBOTAREVA, N.A., LYUBAREV, A.E. AND KURGANOV, B.I. (1998). Study of self-association of muscle glycogen phosphorylase *b* by sedimentation equilibrium methods. *Biochemical Society Transactions* **26**, 766–769.

CHEBOTAREVA, N.A., HARDING, S.E. AND WINZOR, D.J. (2001). Ultracentrifugal studies of the effect of molecular crowding by trimethylamine N-oxide on the self-association of muscle glycogen phosphorylase *b*. *European Journal of Biochemistry* **268**, 506–513.

DEMCHENKO, A.P. (1988). *Luminescence and dynamics of protein structure.* Kiev: Naukova Dumka (in Russian).

DOMBRADI, V. (1981). Structural aspects of catalytic and regulatory function of glycogen phosphorylase. *International Journal of Biochemistry* **13**, 125–139.

ERONINA, T.B., KURGANOV, B.I., LIVANOVA, N.B., CHEBOTAREVA, N.A., PEKEL, N.D. AND POGLAZOV, B.F. (1992). Quantitative method of the estimation of affinity of ligand to enzyme on the basis of the data on digestion by proteolytic enzymes. Binding of FMN to muscle glycogen phosphorylase. *Doklady Akademii Nauk SSSR* **325,** 167–170.

ERONINA, T.B., LIVANOVA, N.B., CHEBOTAREVA, N.A., KURGANOV, B.I., LUO, S. AND GRAVES, D.J. (1996). Deimination of glycogen phosphorylas *b* by peptidylarginine deiminase. Influence on the kinetic characteristics and dimer–tetramer transition. *Biochimie* **78**, 253–258.

GONNELI, M. AND STRAMBINI, G.B. (1995). Phosphorescence lifetime of tryptophan in proteins. *Biochemistry* **34**, 13847–13857.

GUNAR, V.I., SUGROBOVA, N.P., CHEBOTAREVA, N.A., STEPANOVA, S.V., POZNANSKAYA, A.A. AND KURGANOV, B.I. (1990). Synthesis of pyridoxal 5'-phosphate analogs and their interaction with apoenzyme of glycogen phosphorylase *b*. In: *Enzymes dependent on pyridoxal phosphate and other carbonyl compounds as cofactors*. Eds. T. Fukui, H. Kagamiyama, K. Soda and H. Wada, pp 417–419. Oxford: Pergamon Press.

HASCHKE, R.H., HEILMEYER, L.M.G., JR., MEYER, F. AND FISCHER, E.H. (1970). Control of phosphorylase activity in a muscle glycogen particle. III. Regulation of phosphorylase phosphatase. *Journal of Biological Chemistry* **245**, 6657–6663.

HEDRICK, J.L., SHALTIEL, S.H. AND FISCHER, E.H. (1966). On the role of pyridoxal 5'-phosphate in phosphorylase. III. Physicochemical properties and reconstitution of apophosphorylase *b*. *Biochemistry* **8**, 2422–2429.

HEILMEYER, L.M.G., JR., MEYER, F., HASCHKE, R.H. AND FISCHER, E.H. (1970). Control of phosphorylase activity in a muscle glycogen particle. II. Activation by calcium. *Journal of Biological Chemistry* **245**, 6649–6656.

HELMREICH, E.J.M. (1992). How pyridoxal 5'-phosphate could function in glycogen phosphorylase catalysis. *BioFactors* **3**, 159–172.

HELMREICH, E.J.M. AND CORI, C.F. (1964). The role of adenylic acid in the activation of phosphorylase. *Proceedings of the National Academy of Sciences of the United States of America* **51**, 131–138.

HO, H.C. AND WANG, J.H. (1973). A calorimetric study of the interactions between phosphorylase b and its nucleotide activators. *Biochemistry* **12,** 4750–4756.

JOHNSON, L.N., HAJDU, J., ACHARYA, K.R., STUART, D.I., MCLAUGHLIN, P.J., OIKONOMAKOS, N.G. AND BARFORD, D. (1992). Glycogen phosphorylase *b*. In: *Allosteric enzymes*. Ed. G. Herve, pp 81–127. Boca Raton, FL: CRC Press.

KASTENSCHMIDT, L.L., KASTENSCHMIDT, J. AND HELMREICH, E. (1968). The effect of temperature on the allosteric transitions of rabbit muscle phosphorylase *b*. *Biochemistry* **7**, 4543–4556.

KASVINSKY, P.J., MADSEN, N.B., FLETTERICK, R.J. AND SYGUSCH, J. (1978). X-ray crystallographic and kinetic studies of oligosaccharide binding to phosphorylase. *Journal of Biological Chemistry* **253**, 1290–1296.

KLINOV, S.V. AND KURGANOV, B.I. (1994). Kinetic mechanism of activation of muscle glycogen phosphorylase *b* by adenosine 5'-monophosphate. *Archives of Biochemistry and Biophysics* **312**, 14–21.

KLINOV, S.V. AND KURGANOV, B.I. (1995). Specificity of inhibition of muscle glycogen phosphorylase *b* by flavins. *Biochemistry and Molecular Biology International* **35**, 643–650.

KLINOV, S.V., CHEBOTAREVA, N.A., KURGANOV, B.I., LITVAK, ZH.I., ZHILINA, T.A., GLEBOVA, G.D., PEKEL, N.D. AND BEREZOVSKII, V.M. (1984). The interaction of muscle glycogen phosphorylase *b* with flavin mononucleotide and its analogues. *Bioorganicheskaya Khimiya* **10**, 1161–1170.

KLINOV, S.V., KURGANOV, B.I., PEKEL, N.D. AND BEREZOVSKII, V.M. (1986a). Inhibition of muscle glycogen phosphorylase *b* by vitamin B_2 and its coenzyme forms. *Biochemistry International* **13**, 139–145.

KLINOV, S.V., KURGANOV, B.I., PEKEL, N.D. AND BEREZOVSKII, V.M. (1986b). A spectrophotometric study of vitamin B_2 and its coenzyme forms binding to muscle glycogen phosphorylase *b*. *Biochemistry International* **13**, 227–232.

KLINOV, S.V., KURGANOV, B.I., CHEBOTAREVA, N.A., ZHILINA, T.A., LITVAK, ZH.I., GLEBOVA, G.D. AND BEREZOVSKII, V.M. (1988). The interaction of muscle glycogen phosphorylase *b* with riboflavin, its tetraacetyl derivative and their analogues. *Bioorganicheskaya Khimiya* **14**, 1027–1033.

KLINOVA, N.I., KLINOV, S.V., KURGANOV, B.I., MIKHNO, C.D., BALYAKINA, M.V., BELOZEROVA, E.V., RUDAKOVA, I.P., YURKEVICH, A.M. AND GUNAR, V.I. (1988). *Bioorganicheskaya Khimiya* **14**, 1520–1523.

KURGANOV, B.I. (1982). *Allosteric enzymes: kinetic behaviour.* Chichester: John Wiley & Sons.

KURGANOV, B.I., SCHORS, E.I., LIVANOVA, N.B., CHEBOTAREVA, N.A., ERONINA, T.B., ANDREEVA, I.E., MAKEEVA, V.P. AND PEKEL, N.D. (1993). Effect of flavins on the rate of proteolytic digestion of muscle glycogen phosphorylas *b*. *Biochimie* **75**, 481–485.

KURGANOV, B.I., KLINOV, S.V. AND CHEBOTAREVA, N.A. (1994a). Interaction of muscle glycogen phosphorylase *b* with flavins. *Uspekhi Biologicheskoi Khimii* **34**, 83–110.

KURGANOV, B.I., SCHORS, E.I., LIVANOVA, N.B., ERONINA, T.B. AND CHEBOTAREVA, N.A. (1994b). Slow conformational changes in muscle glycogen phosphorylase b induced by specific ligands. *Biochemistry (Moscow)* **59**, 405–410.

KURGANOV, B.I., FEDURKINA, N.V., MITSKEVICH, L.G., MAZHUL, V.M., ZAITSEVA, E.M. AND POGLAZOV, B.F. (1999). Study of muscle glycogen phosphorylase *b* association by means of tryptophan phosphorescence at room temperature. *Doklady Biophysics* **367**, 67–70.

LIVANOVA, N.B. AND KORNILAEV, B.A. (1996). Structure, regulation and denaturation of rabbit muscle glycogen phosphorylase *b*. *Biochemistry (Moscow)* **61**, 1432–1442.

LOWRY, O.H., SCHULZ, D.W. AND PASSONNEAU, J.V. (1967). The kinetics of glycogen phosphorylase from brain and muscle. *Journal of Biological Chemistry* **242**, 271–280.

MADSEN, N.B. AND SHECHOSKY, S. (1967). Allosteric properties of phosphorylase *b*. II. Comparison with kinetic model. *Journal of Biological Chemistry* **242**, 3301–3307.

MATCO, P., BARTON, C., LOPEZ-MAYORA, O., FIMENUZ, J.S. AND CORTIJO, M. (1984). AMP and IMP binding to glycogen phosphorylase *b*. A calorimetric and equilibrium dialysis study. *Journal of Biological Chemistry* **259**, 9384–9390.

MAZHUL, V.M., CHERNITSKII, E.A. AND KONEV, S.V. (1970). Conformation transitions of native proteins in solution and in cells. *Biofizika* **15**, 5–11.

MAZHUL, V.M., KONEV, S.V., ERMOLAEV, YU.S., MARTYNOVA, M.A., NIKOL'SKAJA, V.P. AND PROKOPOVA, ZH.P. (1983). Study of the equilibrium dynamics of cell protein structure by room temperature tryptophan fluorescence. *Biofizika* **28**, 980–984.

MAZHUL, V.M., MJAKINNIK, I.V. AND VOLKOVA, A.N. (1994). Intramolecular dynamics of structure of alkaline phosphatase. *Society of Photo-Optical Instrumentation Engineers. Proceedings* **2370**, 706–710.

MAZHUL, V.M., ZAITSEVA, E.M., MITSKEVICH, L.G., FEDURKINA, N.V. AND KURGANOV, B.I. (1999). Phosphorescence analysis of the intramolecular dynamics of muscle glycogen phosphorylase *b*. *Biophysics (Moscow)* **44**, 975–981.

MERINO, C.G., GARCIA BLANCO, F., POCOVI, M., MENENDEZ, M. AND LAYNEZ, J. (1980). Regulation of phosphorylase *b* by AMP. *Journal of Biochemistry* **87**, 1483–1490.

METZGER, B., HELMREICH, E. AND GLASER, L. (1967). The mechanism of activation of skeletal muscle phosphorylase *a* by glycogen. *Proceedings of the National Academy of Sciences of the United States of America* **57**, 994–997.

MEYER, F., HEILMEYER, L.M.G., JR., HASCHKE, R.H. AND FISCHER, E.H. (1970). Control of phosphorylase activity in a muscle glycogen particle. I. Isolation and characterization of the protein–glycogen complex. *Journal of Biological Chemistry* **245**, 6642–6648.

MONOD, J., WYMAN, J. AND CHANGEUX, J.-P. (1965). On the nature of allosteric transitions: a plausible model. *Journal of Molecular Biology* **12**, 88–118.

MUNOS, F., VALLES, M., DONOSO, J., ECHEVARRIA, G. AND BLANCO, F.G. (1983). Kinetic and thermodynamic study of the tetramerization equilibrium of phosphorylase *b*. *Journal of Biochemistry* **94**, 1649–1661.

OIKONOMAKOS, N.G., SOTIROUDIS, T.G. AND EVANGELOPOULOS, A.E. (1979). Interaction of phosphorylase *b* with eosin: influence of substrates and effectors on eosin–enzyme complexes. *Biochemical Journal* **181**, 309–320.

OIKONOMAKOS, N.G., ACHARYA, K.R. AND JOHNSON, L.N. (1992). Rabbit muscle glycogen

phosphorylase *b*. The structural basis of activation and catalysis. In: *Post-translational modifications of proteins.* Eds. J.J. Harding and M.J.C. Crabbe, pp 81–151. Boca Raton, FL: CRC Press.

REICH, J.G., WANGERMANN, G., FALCK, M. AND ROHDE, K. (1972). A general strategy for parameter estimation from isosteric and allosteric kinetic data and binding measurements. *European Journal of Biochemistry* **26**, 368–379.

SCHORS, E.I., KURGANOV, B.I., LIVANOVA, N.B., CHEBOTAREVA, N.A. AND PEKEL, N.D. (1991). Quantitative method of the estimation of affinity of ligand to enzyme on the basis of the data on digestion by proteolytic enzymes. Binding of FMN to muscle glycogen phosphorylase *b*. *Doklady Akademii Nauk SSSR* **319**, 246–249.

SEALOCK, R.W. AND GRAVES, D.J. (1967). Effect of salt solution on glycogen phosphorylase. A possible role of the phosphoryl group in phosphorylase *a*. *Biochemistry* **6**, 201–207.

SILONOVA, G.V. AND KURGANOV, B.I. (1970). Study of phosphorylase *b* from rabbit skeletal muscles by kinetic method. *Molecular Biology (Moscow)* **4**, 445–459.

SILONOVA, G.V. AND LISOVSKAYA, N.P. (1967). On dimerization of phosphorylase *b*. *Doklady Akademii Nauk SSSR* **17**, 713–720.

SOLOVYEVA, G.A., BARANOVA, L.A., SUNDUKOV, S.YU. AND KHVOROV, YU.V. (1991). Interaction of rabbit skeletal muscle glycogen synthase with substrate analogs: oxo-UDP hydrazones. *Biochemistry (Moscow)* **56**, 1812–1821.

SPRANG, S., FLETTERICK, R., STERN, M., YANG, D., MADSEN, N. AND STURTEVANT, J. (1982). Analysis of an allosteric binding site: the nucleoside inhibitor site of phosphorylase *a*. *Biochemistry* **21**, 2036–2048.

STAFFORD, W.F. (1992). Methods for obtaining sedimentation coefficient distributions. In: *Analytical ultracentrifugation in theory and experiment.* Eds. S.E. Harding, A.J. Rowe and J.C. Horton, pp 359–393. Cambridge, UK: Royal Society of Chemistry.

STEINBERG, I.Z. AND SCHACKMAN, H.K. (1966). Ultracentrifugation studies with absorption optics. V. Analysis of interacting systems involving macromolecules and small molecules. *Biochemistry* **5**, 3728–3747.

STRAMBINI, G.B. (1989). Tryptophan phosphorescence as a monitor of protein flexibility. *Journal of Molecular Liquids* **42**, 155–165.

STURA, E.A., ZANOTTI, G., BABU, Y.S., SANSOM, M.S.P., STUART, D.I., WILSON, K.S. AND JOHNSON, L.N. (1983). Comparison of AMP and NADH binding to glycogen phosphorylase b. *Journal of Molecular Biology* **170**, 529–565.

SZARKA, A., GABELLIERI, E., GONELLI, M., CIONI, P., LAKOS, Z.S. AND SOMOGYI, B. (1998). Alteration of the intramolecular dynamics of glycogen phosphorylase *b* by allosteric ligands. *Photochemistry and Photobiology B: Biology* **42**, 52–56.

VANDERKOI, J.M. AND BERGER, J.M. (1989). Exited triplet states used to study biological macromolecules at room temperature. *Biochimica et Biophysica Acta* **976**, 1–27.

WANG, J.H., KWOK, S.C.,WRICH, E. AND SUZUKI, I. (1970). Distinct AMP binding sites in glycogen phosphorylase *b* as revealed by calorimetric studies. *Biochemical and Biophysical Research Communications* **40**, 1346–1347.